Supporting Information for

Fluorescent probes guided by new practical performance regulation strategy to monitor glutathione in living systems

Mengyao She, [‡a, b] Zhaohui Wang, [‡a] Tianyou Luo, [a] Bing Yin, [a] Ping Liu, [a] Jing Liu, [b] Fulin Chen, [b, *] Shengyong Zhang, [a] and Jianli Li [a, *]

[a] Ministry of Education Key Laboratory of Synthetic and Natural Functional Molecule Chemistry, College of Chemistry & Materials Science, Northwest University, Xi'an, Shaanxi 710127, P. R. China.

[b] Key Laboratory of Resource Biology and Modern Biotechnology in Western China, Ministry of Education, Northwest University, 229 TaiBai North Road, Xi'an, Shaanxi Province, 710069, PR China.

1. Experimental procedures and characterisation data

1.1 Materials

The absorbance spectra were measured on a Shimadzu UV-1700 spectrophotometer. Fluorescent spectra data were recorded by a Hitachi F-4500 fluorescence spectrophotometer equipped with a xenon discharge lamp and 1 cm quartz cell. NMR spectra were collected on a Bruker-AVANCE III 400 MHz spectrometer (at 400 MHz for ^{1}H and 100 MHz for ^{13}C) using tetramethylsilane (TMS) as the internal standard. Mass spectra were performed with Bruker micrOTOF-Q II ESI-Q-TOF LC/MS/MS Spectroscopy. Bioimaging of the sensors was performed on an Olympus FV1000 confocal microscope and the excitation wavelength was set at 488 nm. Flow cytometric analysis was carried out on BD Biosciences AccuriC6 and live mouse imaging was performed on PerkinElmer Lumina LT Serios III. Isoflurane was used for anesthesia. All the live subjects procedures were conducted in accordance with the Experimental Animal Administration regulations issued by the State Committee of Science and Technology of the People's Republic of China and Experiments were approved by the Animal Ethics Committee of Northwest University.

Fluorescein, cinnamic acid derivates, amino acids, α-lipoic acid, and N-Ethylmaleimide were obtained from TCI (Shanghai) Development Co., Ltd. Analytical thin layer chromatography was performed using Merck 60 GF254 silica gel (pre-coated sheets, 0.25 mm thick). Silica gel (0.200-0.300 mm, 60 A, *J&K* Scientific Ltd.) was used for column chromatography.

1.2 Synthesis and characterization of all probes

Fluorescein was acidize with 4 mol/L hydrochloric acid, and dry it in a vacuum oven at 60 ^{o}C for 4 hours for subsequent synthesis. 0.1 mmol cinnamic acid derivatives were acylated by thionyl chloride (0.2 mmol) in 50 ml dichloromethane at 0 ^{o}C and stirred for 5 h, remove the solvent and thionyl chloride by vacuum, and add 0.2 mmol triethylamine and stirred for 0.5 h, then the aforementioned acidize fluorescein (0.1 mmol) were suspended in 20 ml dichloromethane and dropped into to the solution in 1 h. The mixture were stirred for another 6 h at 0 ^{o}C, then remove the solvent, and purified by column chromatography using dichloromethane : methanol (v/v) = 30:1 as eluent.

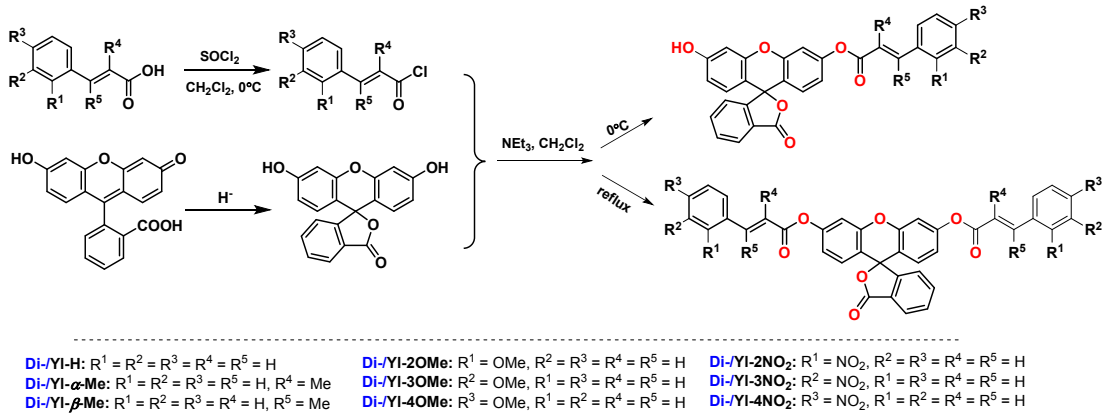

SCHEME S1. Synthesis route of all probes

The characterization data were shown as followed:

Fl-H: white powder, yield: 83.35 %.

^{1}H NMR (400 MHz, d^6-DMSO, TMS) δ 10.26 (s, 1H), 8.06 (d, *J* = 7.6 Hz, 1H), 7.92 (d, *J* = 16.0 Hz, 1H), 7.85 (t, *J* = 5.8 Hz, 3H), 7.77 (t, *J* = 7.4 Hz, 1H), 7.49 (d, *J* = 4.4 Hz,3H), 7.39 (d, *J* = 7.6 Hz,1H), 7.37 (s, 1H), 7.02 (d, *J* = 8.4 Hz, 1H), 6.94 (d, *J* = 16.0 Hz, 1H), 6.87 (d, *J* = 8.8 Hz, 1H), 6.75 (s, 1H), 6.63 (s, 2H). ^{13}C NMR (100 MHz, d^6-DMSO, TMS) δ 169.0, 165.0, 160.2, 152.8, 152.3, 152.0, 151.7, 147.5, 136.3, 134.2, 131.5, 130.8, 129.6, 129.5, 129.5, 129.2, 126.3, 125.3, 124.6, 118.6, 117.2, 117.1, 113.6, 110.9, 109.6, 102.8, 82.5, 55.4. EMS/MS m/z calcd. for $C_{29}H_{17}O_6^-$ ([M-H]$^-$): 461.1031, found 461.1035.

Fl-*α*-Me: flaxen powder, yield: 79.41 %.

^{1}H NMR (400 MHz, $(CD_3)_2CO$, TMS) 8.03 (d, *J* = 7.6 Hz, 1H), 7.05 (s, 1H), 7.85 (t, *J* = 7.6 Hz, 1H), 7.78 (t, *J* = 7.6 Hz, 1H), 7.59 (d, *J* = 7.6 Hz, 2H), 7.50 (d, *J* = 7.6 Hz, 2H), 7.44 (d, *J* = 7.6 Hz, 1H), 7.38 (d, *J* = 7.6 Hz, 1H), 7.30 (s, 1H), 7.03 (d, *J* = 8.4 Hz, 1H), 6.94 (d, *J* = 8.4 Hz, 1H), 6.81 (s, 1H), 6.72 (q, *J* = 8.4 Hz, 2H), 2.24 (s, 3H). ^{13}C NMR (100 MHz, $(CD_3)_2CO$, TMS) δ 168.49, 166.14, 159.56, 152.96, 152.79, 152.20, 151.76, 140.64, 138.39, 135.44, 135.39, 130.10, 129.90, 129.64, 129.33, 129.06, 128.92, 128.57, 128.44, 127.37, 126.63, 124.67, 124.09, 117.98, 117.07, 112.80, 110.38, 102.49, 81.94, 13.57. EMS/MS m/z calcd. for $C_{30}H_{19}O_6^-$ ([M-H]$^-$): 475.1187, found 475.1311

Fl-*β*-Me: flaxen powder, yield: 88.47 %.

^{1}H NMR (100 MHz, $CDCl_3$, TMS) 8.02 (d, *J* = 6.8 Hz, 1H), 7.63 (quint, *J* = 5.6 Hz, 2H), 7.55 (d, J = 3.6 Hz, 2H), 7.43 (d, *J* = 3.2 Hz, 2H), 7.14 (s, 1H), 7.07 (d, *J* = 7.6 Hz, 1H), 6.82 (q, *J* = 8.4 Hz, 2H), 6.8 (s, 1H), 6.62 (d, *J* = 8.8 Hz, 1H), 6.52 (d, *J* = 6.8 Hz, 1H), 6.38 (s, 1H), 6.28 (s, 1H), 2.65 (s, 3H). ^{13}C NMR (100 MHz, $CDCl_3$, TMS) δ 170.2, 165.1, 160.2, 158.6, 153.1, 152.1, 152.0, 151.9, 141.6, 135.3, 129.9, 129.7,

129.1, 129.1, 128.7, 126.5, 126.4, 125.1, 124.1, 117.6, 116.4, 115.4, 112.8, 110.6, 110.1, 103.1, 83.4, 18.5. EMS/MS m/z calcd. for $C_{30}H_{19}O_6^-$ ([M-H]$^-$): 475.1187, found 475.1162.

Fl-2OMe: flaxen powder, yield: 85.97 %.

^{1}H NMR (400 MHz, $CDCl_3$, TMS) δ 8.19 (d, *J* = 16.4 Hz, 1H), 8.02 (d, *J* = 7.2 Hz, 1H), 7.63 (quint, *J* = 6.8 Hz, 2H), 7.57 (d, *J* = 7.6 Hz, 1H), 7.41 (t, *J* = 7.6 Hz, 1H), 7.16 (s, 1H), 7.08 (d, *J* = 7.2 Hz, 1H), 7.00 (t, *J* = 7.6 Hz, 1H), 6.96 (d, *J* = 8.0 Hz, 1H), 6.83 (dd, J_1 = 14.0 Hz, J_1 = 8.8 Hz, 2H), 6.74 (d, *J* = 16.4 Hz, 1H), 6.69 (s,1H), 6.63 (d, *J* = 8.8 Hz, 1H), 6.53 (d, *J* = 8.4 Hz, 1H), 6.27 (br, 1H), 3.93 (s, 3H). ^{13}C NMR (100 MHz, $(CD_3)_2CO$, TMS) δ 168.5, 164.8, 159.6, 158.7, 152.9, 152.5, 152.2, 151.7, 142.0, 135.4, 132.5, 130.1, 129.3, 129.2, 129.0, 126.6, 124.7, 124.1, 122.6, 120.8, 117.9, 117.0, 116.9, 112.8, 111.6, 110.3, 102.6, 82.0, 55.2. EMS/MS m/z calcd. for $C_{30}H_{19}O_7^-$ ([M-H]$^-$): 491.1136, found 491.1149.

Fl-3OMe: flaxen powder, yield: 87.67 %.

^{1}H NMR (400 MHz, $CDCl_3$, TMS) δ 8.03 (d, *J* = 6.8 Hz, 1H), 8.03 (d, *J* = 6.8 Hz, 1H), 7.87 (d, *J* = 16 Hz, 1H), 7.74 (quint, *J* = 7.2 Hz, 2H), 7.35 (s, 1H), 7.19 (d, *J* = 7.6 Hz, 1H), 7.08-7.12 (m, 2H), 6.99 (d, *J* = 7.6 Hz, 1H), 6.80-6.87 (m, 2H), 6.69 (s, 1H), 6.64 (s, 1H), 6.61 (d, *J* = 5.2 Hz, 1H), 6.53 (d, *J* = 8.8 Hz, 1H), 6.16 (s, 1H), 3.86 (s, 3H). ^{13}C NMR (100 MHz, $(CD_3)_2CO$, TMS) δ 168.5, 164.4, 160.2, 159.6, 152.9, 152.6, 152.4, 152.2, 151.8, 146.9, 135.5, 135.4, 130.1, 130.0, 129.3, 129.1, 126.6, 124.7, 124.1, 121.2, 117.9, 117.1, 117.1, 113.0, 112.9, 110.4, 110.3, 102.6, 82.0, 54.8. EMS/MS m/z calcd. for $C_{30}H_{19}O_7^-$ ([M-H]$^-$): 491.1136, found 491.1173.

Fl-4OMe: yellow powder, yield: 85.42 %.

^{1}H NMR (400 MHz, $CDCl_3$, TMS) δ 8.02 (d, *J* = 6.0 Hz, 1H), 7.86 (d, *J* = 16 Hz, 1H), 7.63 (quint, *J* = 5.8 Hz, 2H), 7.56 (d, *J* = 8.8 Hz, 2H), 7.15 (s, 1H), 7.04 (d, *J* = 5.6 Hz, 1H), 6.95 (d, *J* = 8.8 Hz, 2H), 6.79-6.86 (m, 2H), 6.67 (s, 1H), 6.62 (d, *J* = 8.4 Hz, 1H), 6.48-6.54 (m, 2H), 6.31 (s, 1H), 3.86 (s, 3H). ^{13}C NMR (100 MHz, $(CD_3)_2CO$, TMS) δ 168.51, 164.67, 162.11, 159.57, 152.92, 152.51, 152.20, 151.72, 146.74, 135.39, 130.39, 130.09, 129.82, 129.31, 129.00, 126.75, 126.63, 124.67, 124.09, 117.93, 116.96, 114.45, 114.30, 113.93, 112.82, 110.31, 102.53, 81.99, 54.95. EMS/MS m/z calcd. for $C_{30}H_{19}O_7^-$ ([M-H]$^-$): 491.1136, found 491.1135.

Fl-2NO$_2$: yellow powder, yield: 74.43 %.

^{1}H NMR (400 MHz, $(CD_3)_2CO$, TMS) δ 9.11 (s, *J* = 6.0 Hz, 1H), 8.28 (d, *J* = 16 Hz, 1H), 8.15 (d, *J* = 8.0 Hz, 1H), 8.04 (t, *J* = 8.0 Hz, 2H), 7.86 (q, *J* = 7.6 Hz, 2H), 7.77 (t, *J* = 8.4 Hz, 2H), 7.38 (d, *J* = 8.4 Hz, 1H), 7.30 (s, 1H), 7.03 (d, *J* = 6.4 Hz, 1H), 6.95

(d, *J* = 8.4 Hz, 1H), 6.81 (t, *J* = 8.0 Hz, 2H), 6.70 (q, *J* = 8.8 Hz, 2H). ^{13}C NMR (100 MHz, $(CD_3)_2CO$, TMS) δ 168.45, 163.68, 159.60, 159.49, 152.91, 152.17, 151.76, 148.81, 142.08, 135.40, 133.86, 131.21, 130.11, 129.56, 129.43, 129.32, 129.16, 126.62, 124.84, 124.67, 124.10, 121.48, 117.77, 117.35, 112.86, 112.78, 110.35, 110.26, 102.52, 102.46, 81.88. EMS/MS m/z calcd. for $C_{29}H_{16}NO_8^-$ ([M-H]$^-$): 506.0881, found 506.0913.

Fl-3NO$_2$: yellow powder, yield: 72.94%.

^{1}H NMR (400 MHz, $(CD_3)_2CO$, TMS) δ 9.81 (S, 1H), 8.24 (S, 1H), 7.87 (t, *J* = 8.0 Hz, 2H), 7.62 (d, *J* = 10.0 Hz, 1H), 7.59 (S, 1H), 7.38 (t, *J* = 7.2 Hz, 1H), 7.31 (t, *J* = 7.6 Hz, 2H), 6.92 (t, *J* = 10.0 Hz, 2H), 6.62 (d, *J* = 16.0 Hz, 1H), 6.57 (d, *J* = 8.8H, 1H), 6.42 (d, *J* = 8.4, 1H), 6.29 (s, 1H), 6.17 (s, 2H). ^{13}C NMR (100 MHz, $(CD_3)_2CO$, TMS) δ 168.5, 164.0, 159.7, 152.9, 152.2, 152.2, 151.8, 148.9, 144.3, 143.5, 136.0, 135.4, 134.2, 130.4, 130.1, 129.4, 129.3, 129.2, 126.6, 124.9, 124.7, 124.5, 124.4, 124.1, 123.8, 123.0, 120.8, 120.0, 118.3, 117.8, 117.3, 112.9, 110.3, 102.6. EMS/MS m/z calcd. for $C_{29}H_{16}NO_8^-$ ([M-H]$^-$): 506.0881, found 506.0931.

Fl-4NO$_2$: yellow powder, yield: 76.57 %.

^{1}H NMR (400 MHz, $(CD_3)_2CO$, TMS) 10.28 (s, 1H), 8.31 (d, *J* = 8.8 Hz, 2H), 8.14 (d, *J* = 8.8 Hz, 1H), 8.06 (t, *J* = 7.2 Hz, 2H), 7.87-7.76 (m, 3H), 7.39 (s, 2H), 7.17 (d, *J* = 16 Hz, 1H), 7.04 (d, *J* = 6.8 Hz, 1H), 6.89 (d, *J* = 8.8 Hz, 1H), 6.76 (s, 1H), 6.43(s, 2H). ^{13}C NMR (100 MHz, $(CD_3)_2CO$, TMS) δ 168.50, 163.83, 159.59, 152.89, 152.16, 151.74, 148.82, 144.10, 144.03, 140.31, 135.41, 130.12, 129.49, 129.30, 129.14, 126.60, 124.70, 124.07, 124.01, 121.13, 117.76, 117.30, 112.87, 110.37, 110.25, 102.54, 81.92. EMS/MS m/z calcd. for $C_{29}H_{16}NO_8^-$ ([M-H]$^-$): 506.0881, found 506.0933.

1.3 Theoretical simulation method

DFT calculations have been applied to simulate the recognition process to compare the properties of these probes. All the calculations were performed with functional B3LYP[36] for stable structures and UB3LYP for free radicals, with a combination of double-ζ quality consisting of 6-31G* for C, H elements and 6-31+G** for N, O, S elements on Gaussian 09 Program[37]. The optimized structures were confirmed to be local minimums due to the non-existence of imaginary frequency. The environmental effect was included via the PCM model with water as the solvent molecule.

1.4 Solution preparation procedure

All the reagent grade chemicals consumed in this work were procured from commercial sources and used as received. Stock solutions of all probes (200 μM) were

prepared in DMSO. Stock solutions of all analytes (2 mM) were prepared in 0.1 M PBS, pH=7.4.

To a 10 mL volumetric tube, 1 mL of 200 μM probe and different volume of GSH (2 mM in 0.1M PBS) were added. The mixture was diluted to 10 mL with 0.1 M PBS. Then, 3.0 mL of each solution was transferred to a 1 cm quartz cell. The fluorescence data was recorded between 480 nm-700 nm. The excitation and emission wavelength of slit width were both set at 5.0 nm and the excitation wavelength was set at 470 nm.

2. Optical properties of designed GSH probes

2.1 pH stability

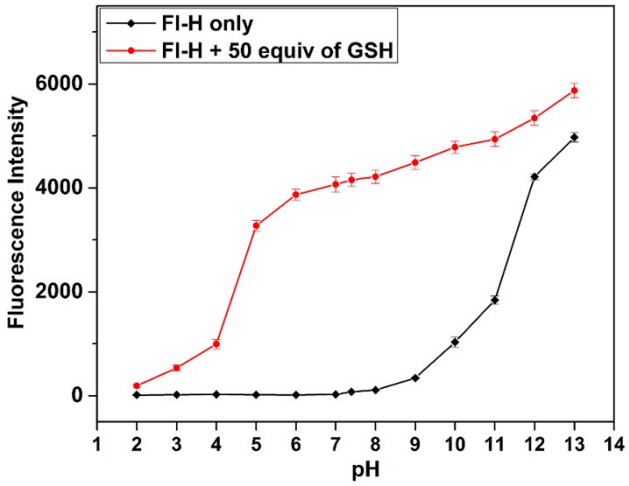

Figure S1. pH stability of **Fl-H**

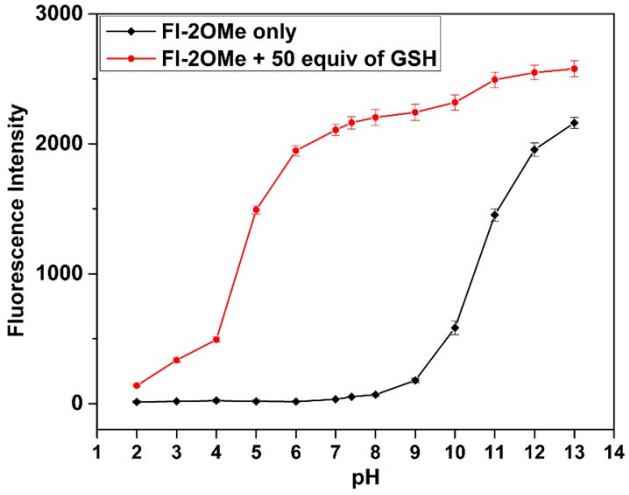

Figure S2. pH stability of **Fl-2OMe**

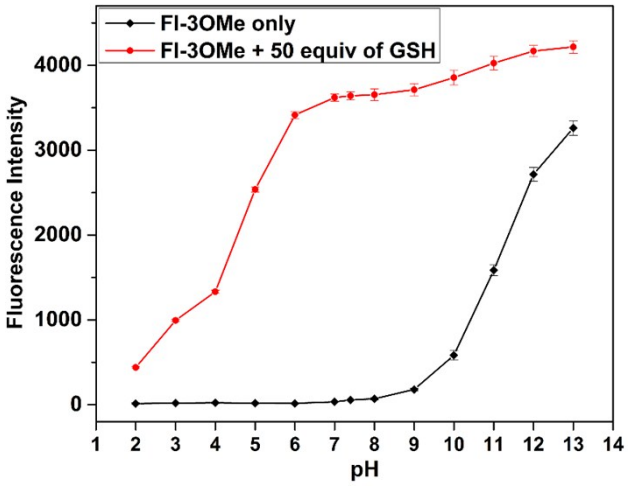

Figure S3. pH stability of **Fl-3OMe**

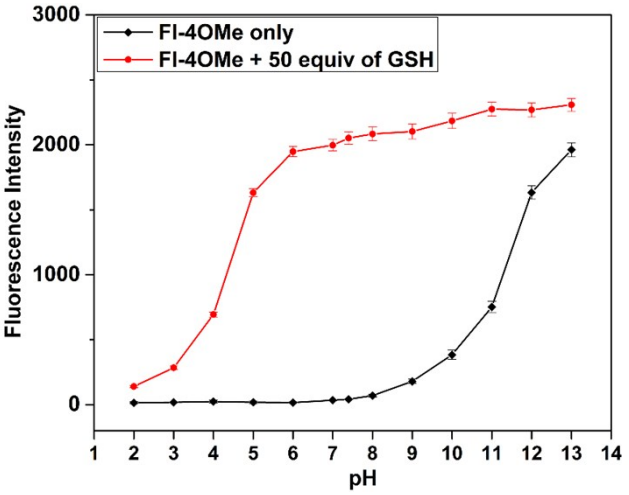

Figure S4. pH stability of **Fl-4OMe**

2.2 selectivity and competition experiments

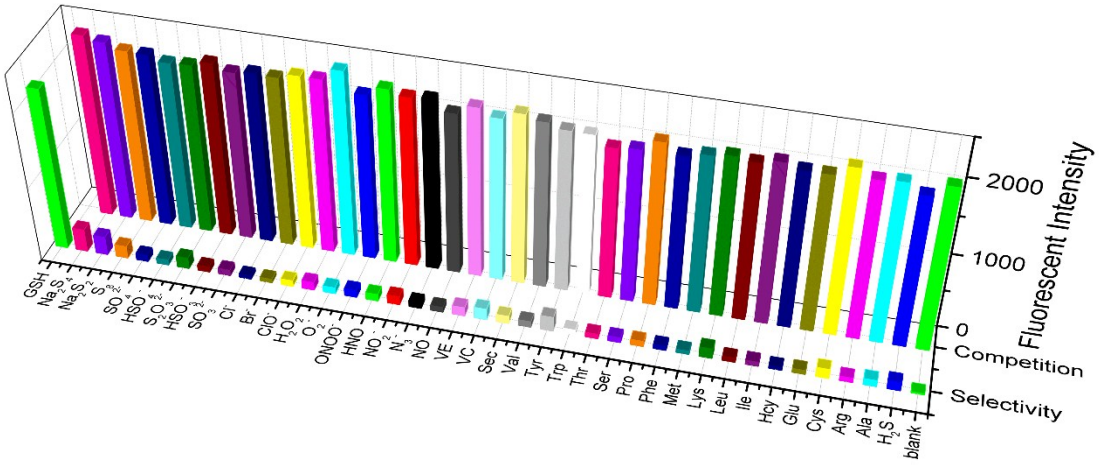

Figure S5. selectivity and competition experiment of **Fl-2OMe**

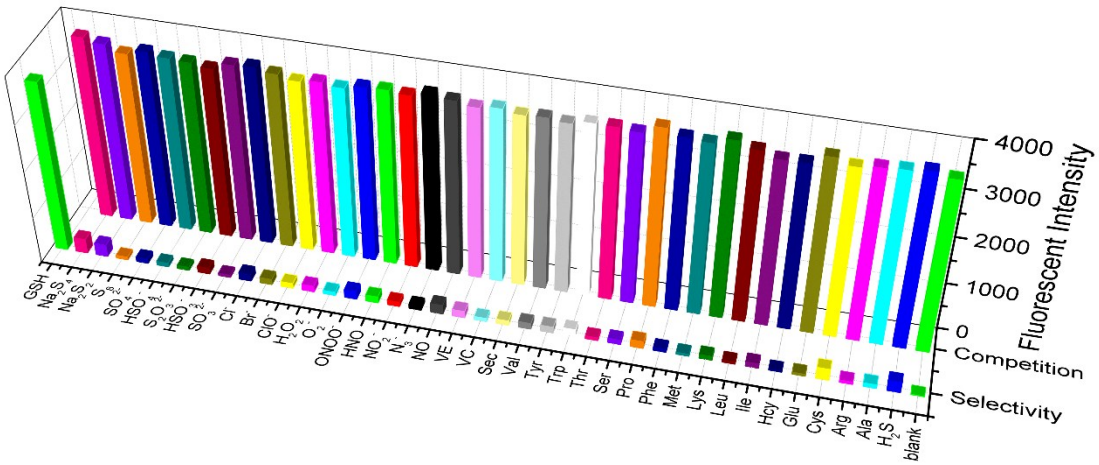

Figure S6. selectivity and competition experiment of **Fl-3OMe**

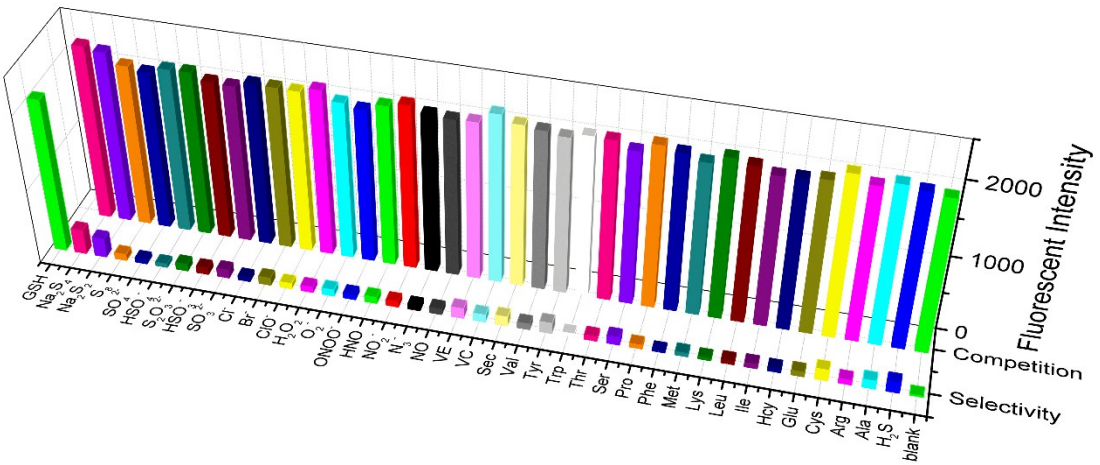

Figure S7. selectivity and competition experiment of **Fl-4OMe**

2.3 Titration experiments

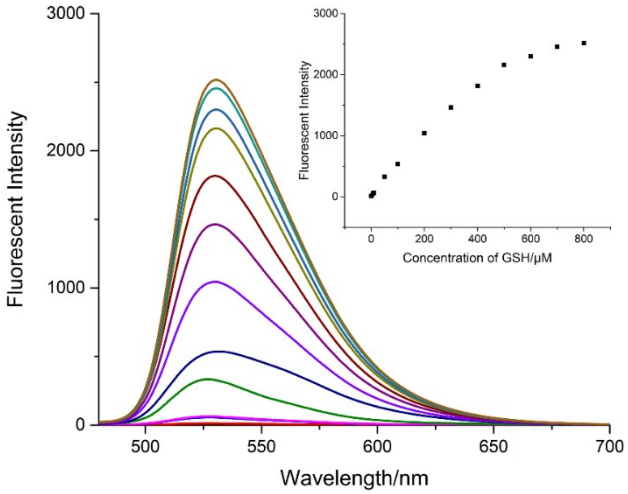

Figure S8. Fluorescence spectrum changes of **Fl-2OMe** upon addition of GSH (0-80 equiv.)

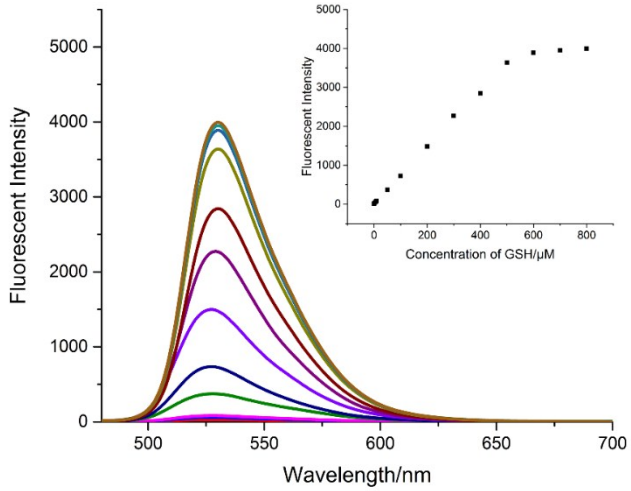

Figure S9. Fluorescence spectrum changes of **Fl-3OMe** upon addition of GSH (0-80 equiv.)

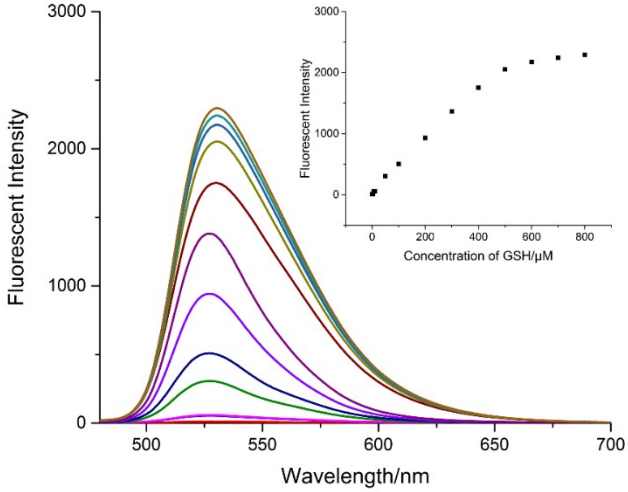

Figure S10. Fluorescence spectrum changes of **Fl-4OMe** upon addition of GSH (0-80 equiv.)

2.4 linear relationship between probes and GSH

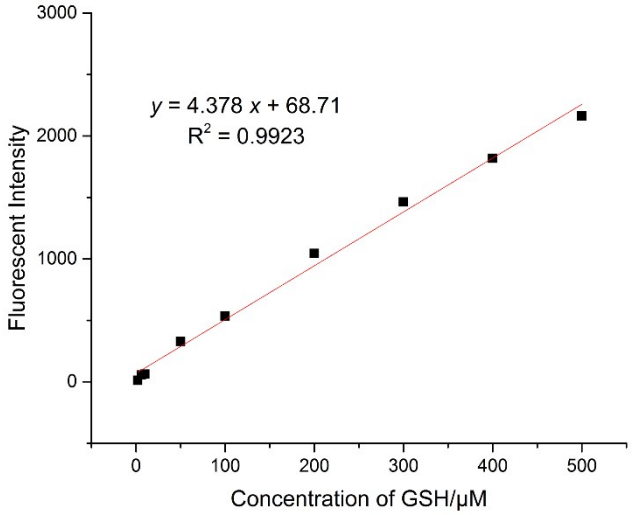

Figure S11. Linear relationship between **Fl-2OMe** and GSH (0-50 equiv.)

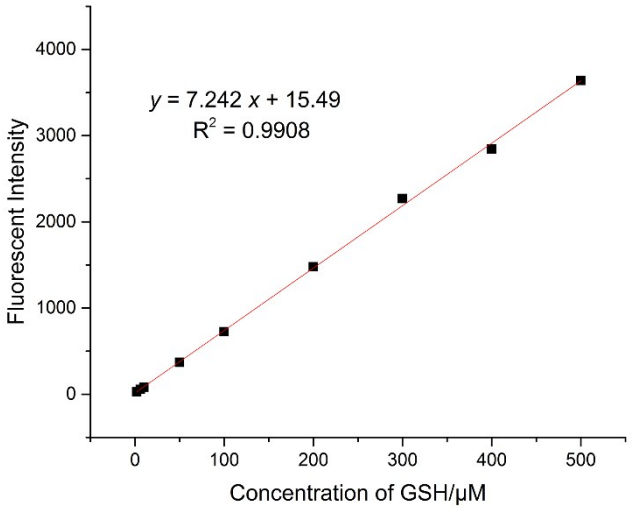

Figure S12. Linear relationship between **Fl-3OMe** and GSH (0-50 equiv.)

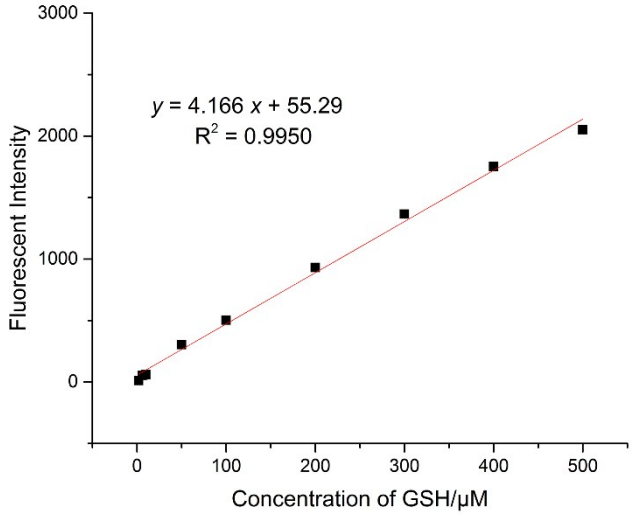

Figure S13. Linear relationship between **Fl-4OMe** and GSH (0-50 equiv.)

2.5 Time-depended experiments

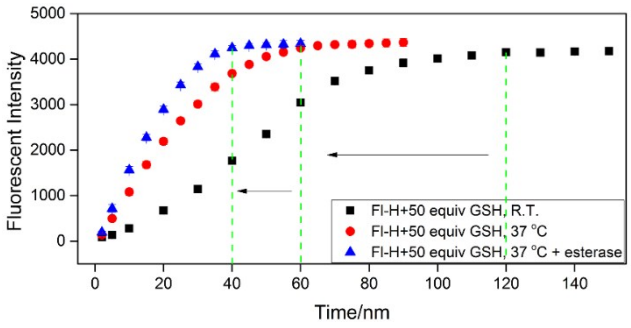

Figure S14 Time-depended experiment of **Fl-H** in room temperature, 37 °C and 37 °C with esterase.

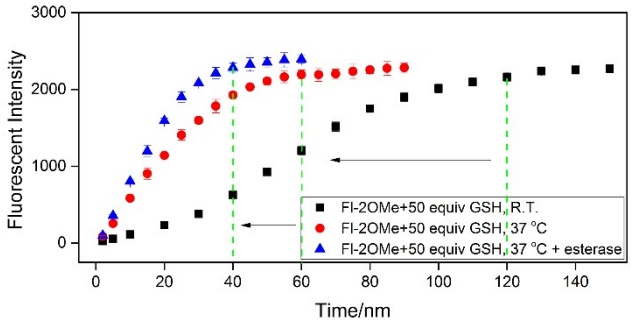

Figure S15 Time-depended experiment of **Fl-2OMe** in room temperature, 37 °C and 37 °C with esterase.

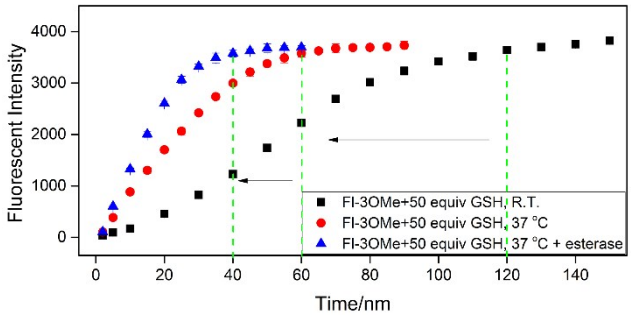

Figure S16 Time-depended experiment of **Fl-3OMe** in room temperature, 37 °C and 37 °C with esterase.

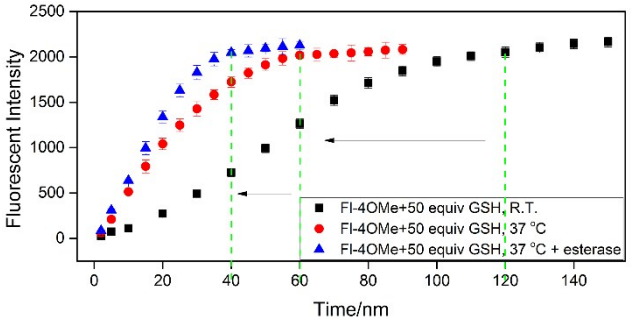

Figure S17 Time-depended experiment of **Fl-4OMe** in room temperature, 37 °C and 37 °C with esterase.

3. Photo stability designed GSH probes

3.1 Photo stability in-vitro

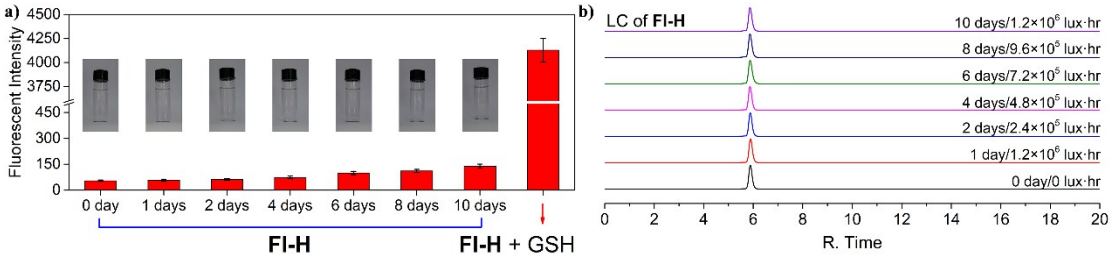

Figure S18 Photo stability of **Fl-H** in-vitro. a) Fluorescent intensity changes; b) LC changes. Under illumination for 10 days with a total illuminance of 1.2 × 10^6 lux·hr.

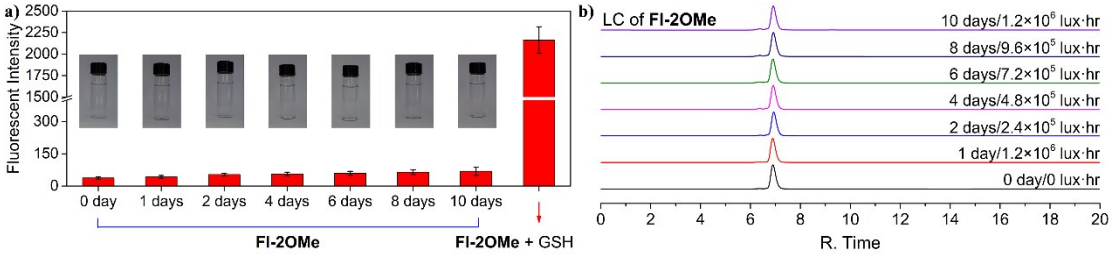

Figure S19 Photo stability of **Fl-2OMe** in-vitro. a) Fluorescent intensity changes; b) LC changes. Under illumination for 10 days with a total illuminance of 1.2 × 10^6 lux·hr.

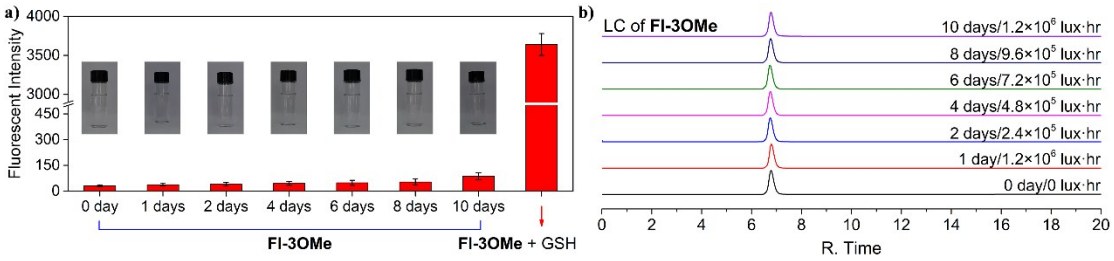

Figure S20 Photo stability of **Fl-3OMe** in-vitro. a) Fluorescent intensity changes; b) LC changes. Under illumination for 10 days with a total illuminance of 1.2 × 10^6 lux·hr.

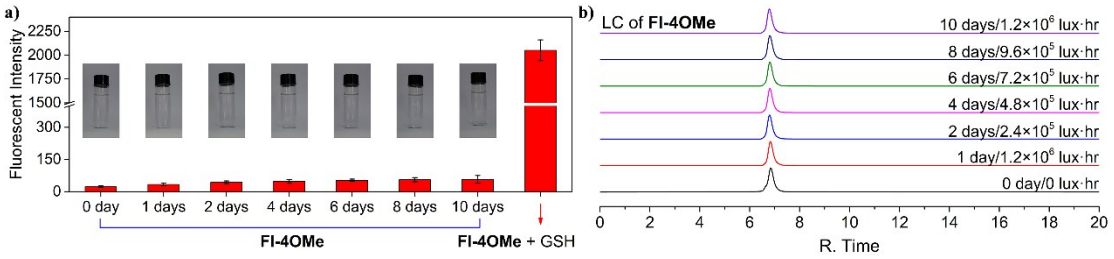

Figure S21 Photo stability of **Fl-4OMe** in-vitro. a) Fluorescent intensity changes; b) LC changes. Under illumination for 10 days with a total illuminance of 1.2 × 10^6 lux·hr.

3.2 Photo stability in cells

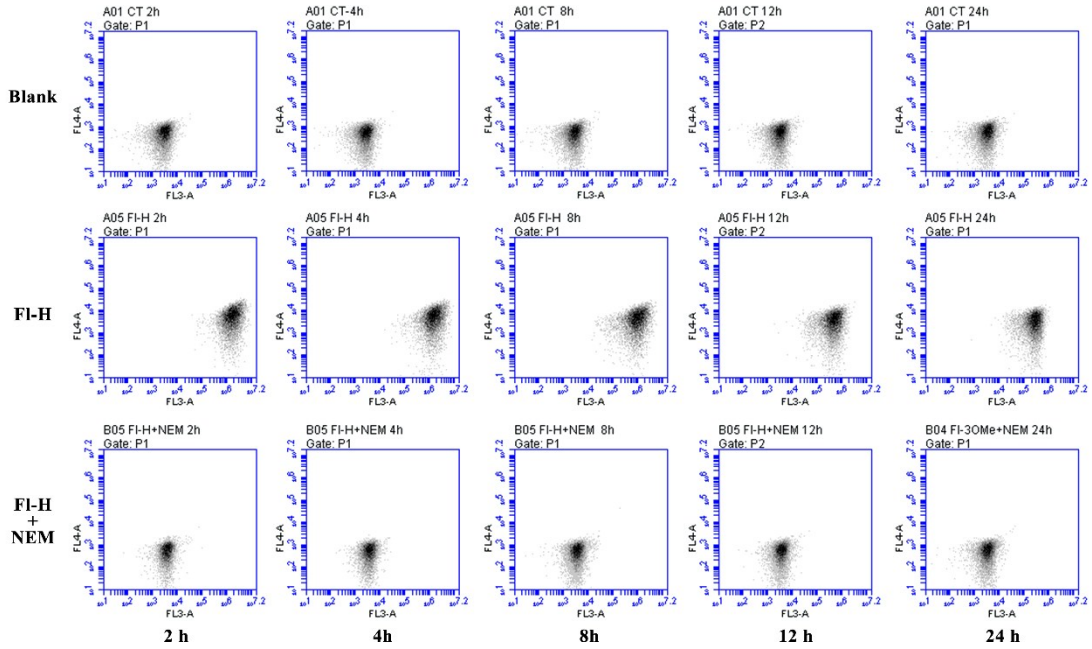

Figure S22 Photo stability scatter diagram of **Fl-H** under illumination in cells by flow cytometry.

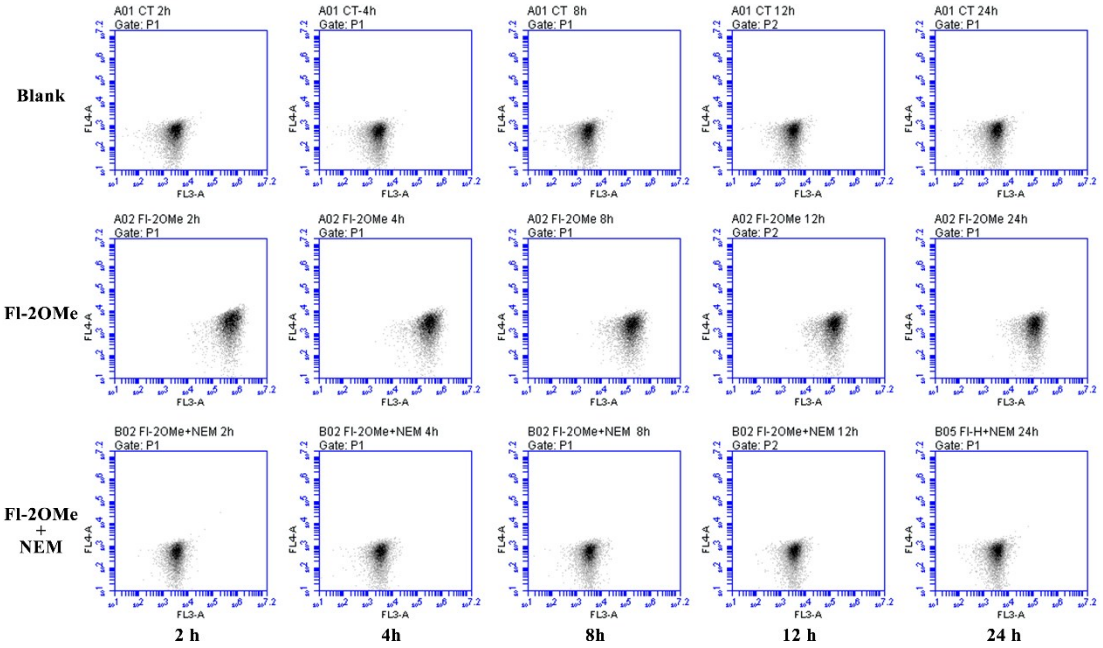

Figure S23 Photo stability scatter diagram of **Fl-2OMe** under illumination in cells by flow cytometry.

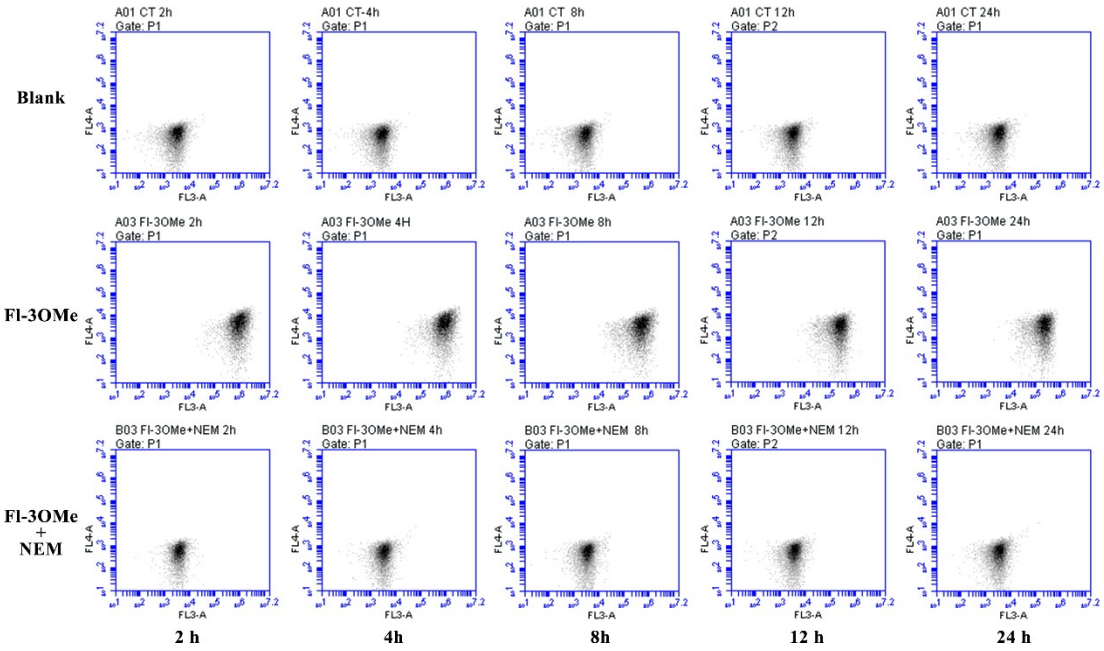

Figure S24 Photo stability scatter diagram of **Fl-3OMe** under illumination in cells by flow cytometry.

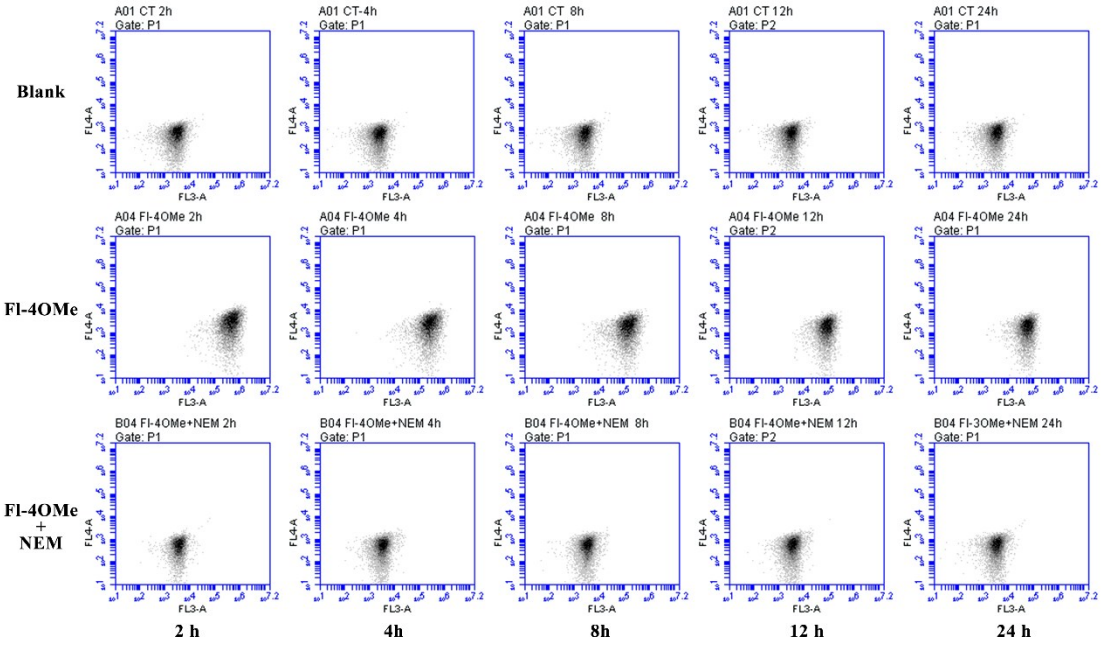

Figure S25 Photo stability scatter diagram of **Fl-4OMe** under illumination in cells by flow cytometry.

4. Cytotoxicity test

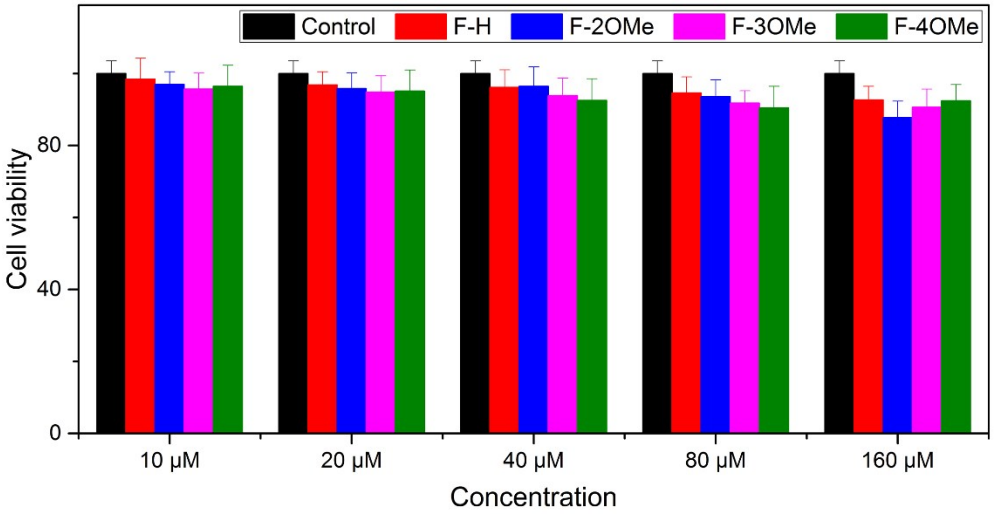

Figure S26. Cell viability on different concentration.

5. Living mice imaging

The positive cell imaging results in MCF-7 cells encouraged us to pursue the suitability of our probes for monitoring GSH in living animals. We used Kunming mice as a model to assess the effectiveness of using probe **Fl-H/2/3/4OMe** to detect GSH in a living organism (Figure S15-S18). Taking **Fl-H** as an example, the mouse was given a hypodermic injection with the pure probe (0.5 mM, in 200 μL PBS buffer solution). After 5 min., an obvious enhancement of fluorescence was observed. The signal intensity increased gradually with time and tended to be stable after about 60 min. By comparison, mice treated with NEM (2 mM, in 100 μL PBS buffer solution) before probe injection showed only a negligible fluorescent emission. Mice treated with *α*-LPA (2 mM, in 100 μL PBS buffer solution) prior to probe injection exhibited more intense fluorescence than the probe-only group. These results suggested that **Fl-H/2/3/4OMe** are sensitive enough to detect basal levels of endogenous GSH produced without stimulation, and could tolerate abnormal GSH concentrations. These experiments have highlighted the utility of **Fl-H/2/3/4OMe** for quantitative detection of GSH in living organisms.

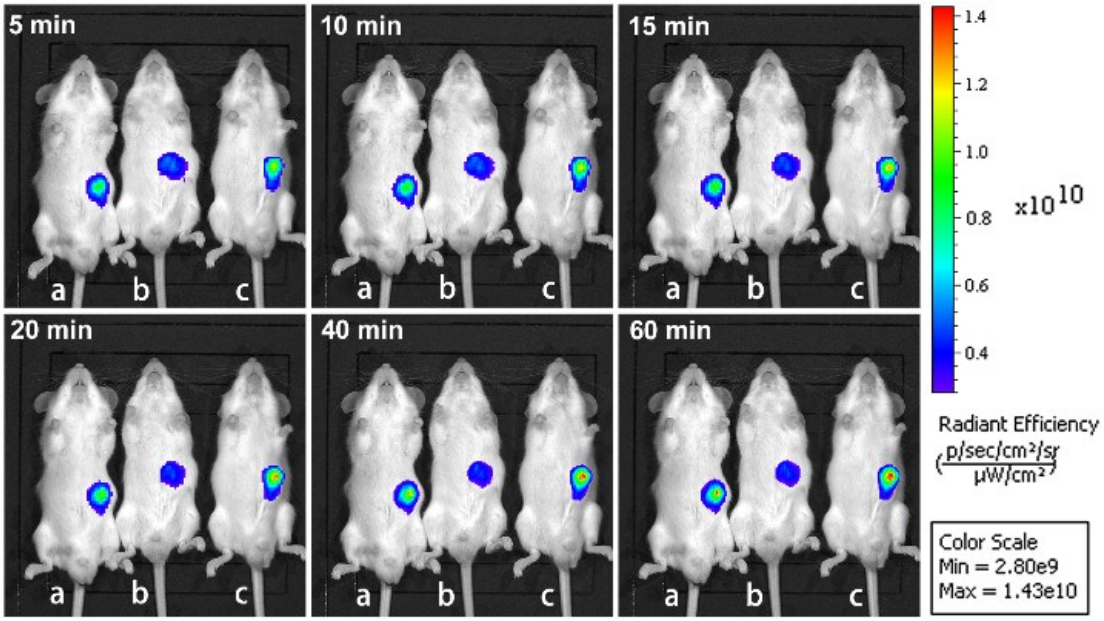

Figure S27. Living Mice imaging of probe **Fl-H**+50 equiv GSH in 60 min. a) Mice inject with 1 mM probe **Fl-H**; b) Mice inject with 2 mM NEM, then inject with 1 mM probe **Fl-H**; c) Mice inject with 2 mM α-LPA, then inject with 1 mM probe **Fl-H**.

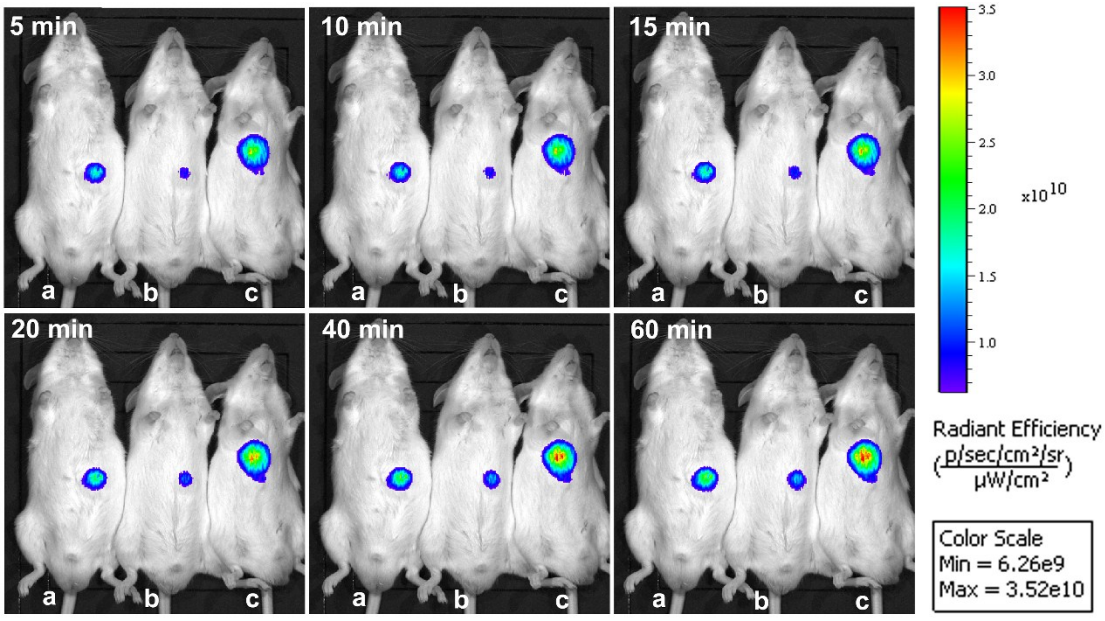

Figure S28. Living Mice imaging of probe **Fl-2OMe**+50 equiv GSH in 60 min. a) Mice injected with 1 mM probe **Fl-2OMe**; b) Mice inject with 2 mM NEM, then inject with 1 mM probe **Fl-2OMe**; c) Mice inject with 2 mM α-LPA, then inject with 1 mM probe **Fl-2OMe**.

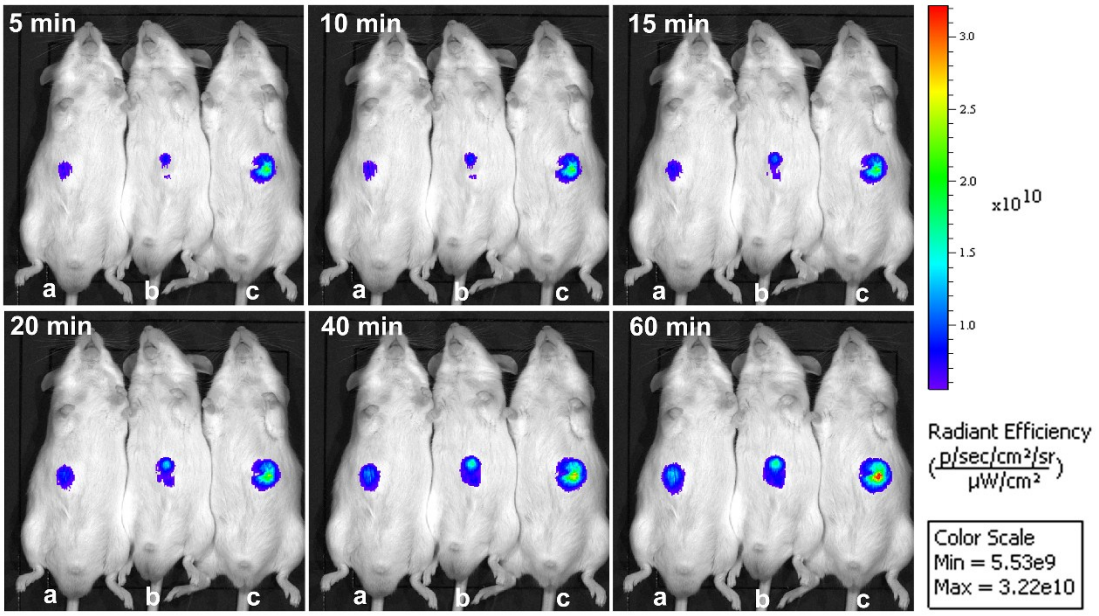

Figure S29. Living Mice imaging of probe **Fl-3OMe**+50 equiv GSH in 60 min. a) Mice injected with 1 mM probe **Fl-3OMe**; b) Mice inject with 2 mM NEM, then inject with 1 mM probe **Fl-3OMe**; c) Mice inject with 2 mM α-LPA, then inject with 1 mM probe **Fl-3OMe**.

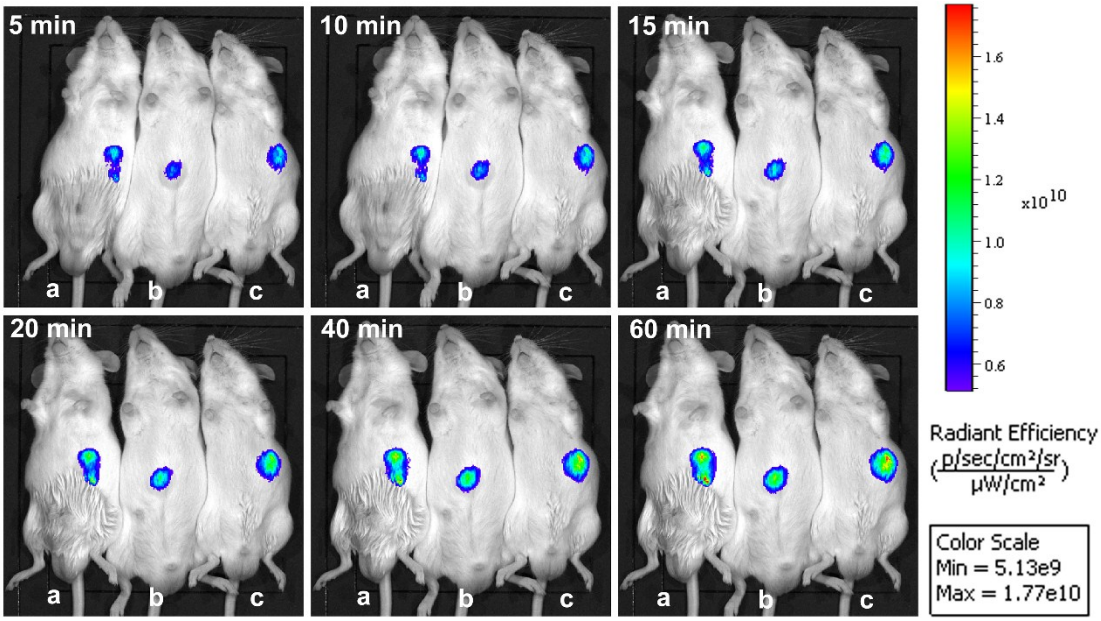

Figure S30. Living Mice imaging of probe Fl-3OMe +50 equiv GSH in 60 min. a) Mice injected with 1 mM probe **Fl-4OMe**; b) Mice inject with 2 mM NEM, then inject with 1 mM probe **Fl-4OMe**; c) Mice inject with 2 mM α-LPA, then inject with 1 mM probe **Fl-4OMe**.

6. Computational details

DFT calculations have been applied to simulate the recognition process by comparing the properties of these probes. All the calculations were performed with B3LYP functional[1] and UB3LYP with a combination of basis of double-ζ quality consisting of 6-31G** for C, H elements, 6-31+G** for N, O, S elements on Gaussian 09 Program[2]. The optimized structures were confirmed to be local minimums due to the non-existence of imaginary frequency, and the environmental effect was included via PCM model with water as the solvent molecule.

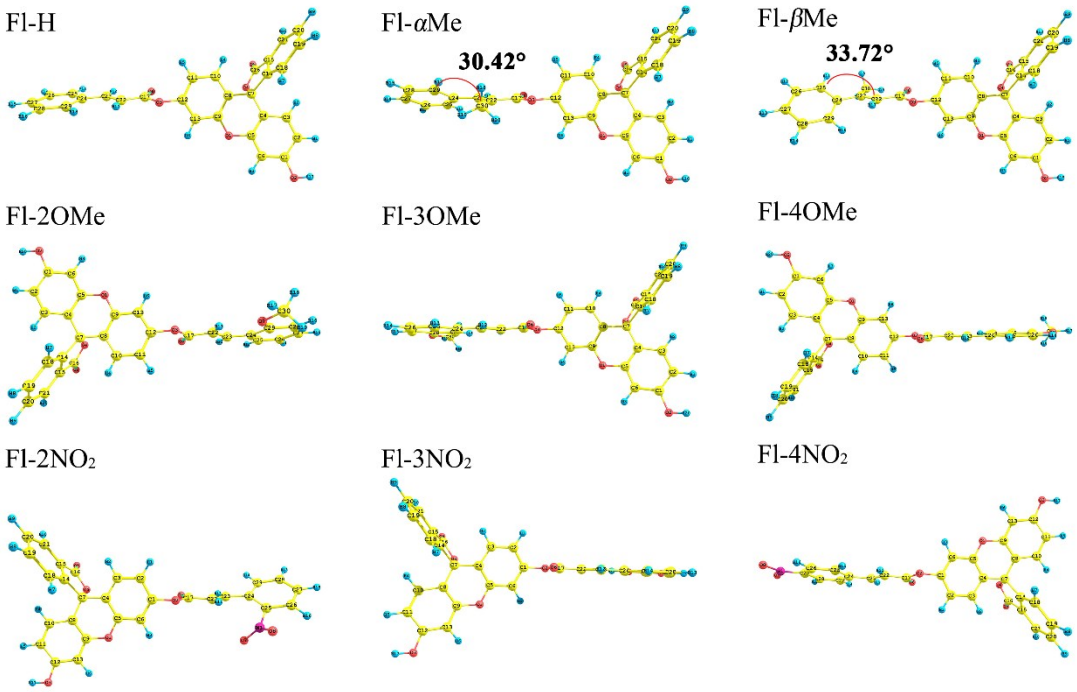

Figure S31. Calculated structure of designed GSH probes.

All these subsequent calculation such as front orbital theory analysis, energies analysis, Fukui function and NBO analysis were all obtained based on these structures.

7. NMR, MS spectra of all synthesized compounds

7.1 NMR spectra of all probes

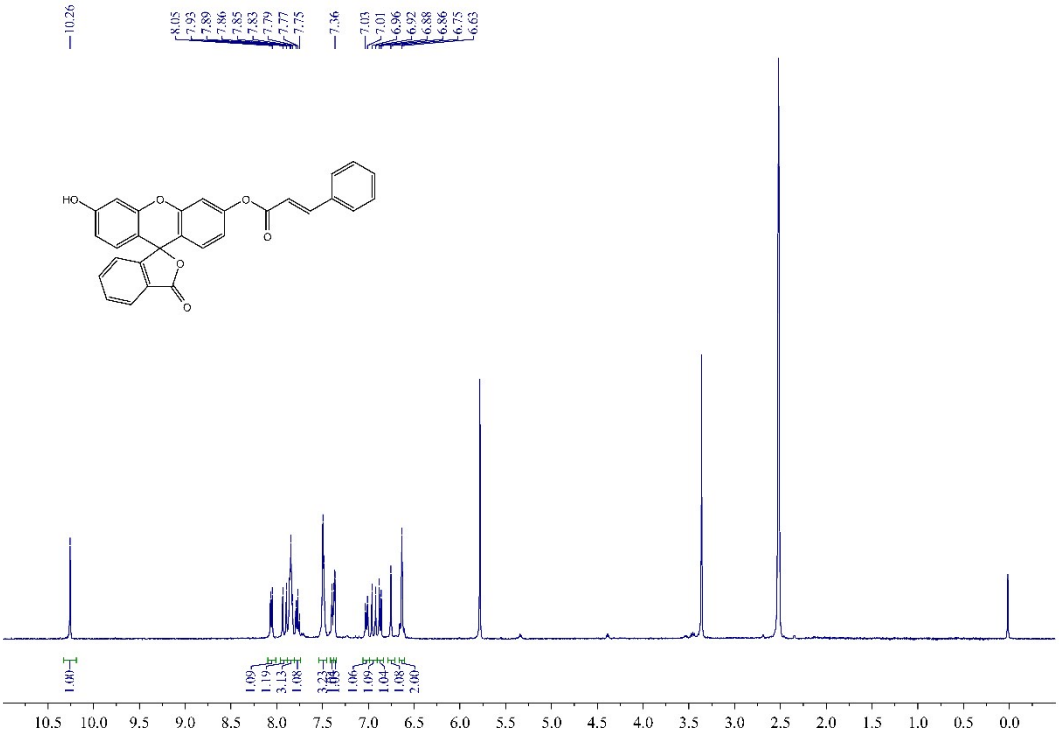

Figure S32. ^{1}H NMR of **Fl-H** in d^{6}-DMSO

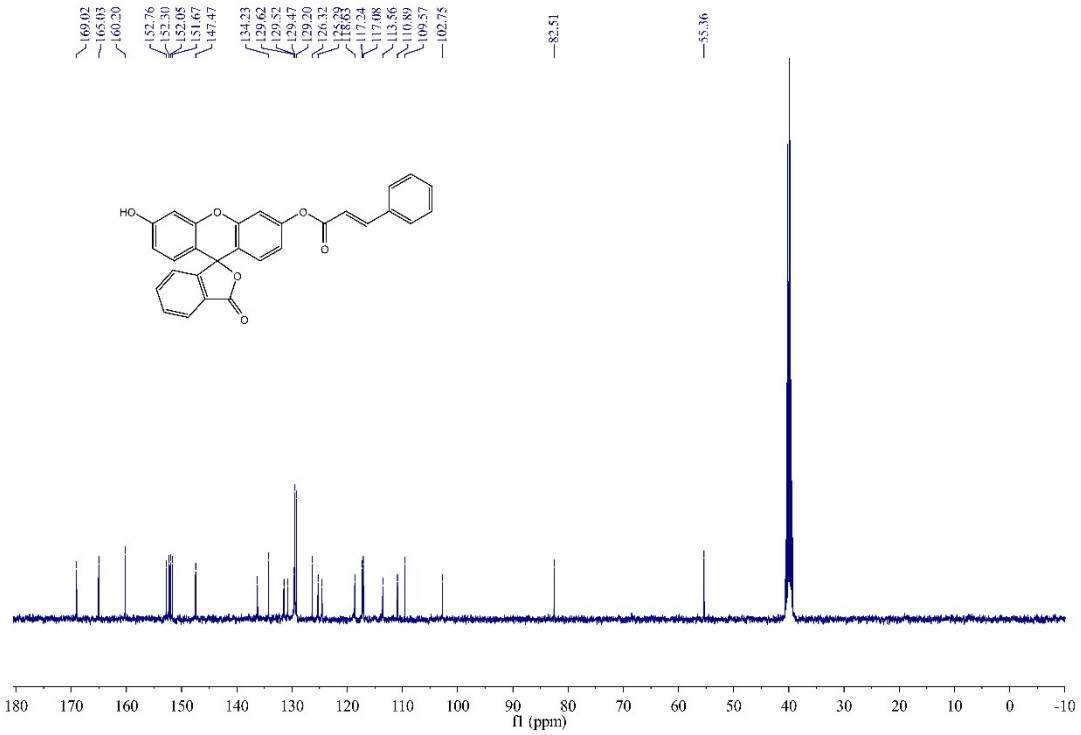

Figure S33. ^{13}C NMR of Fl-H in d^{6}-DMSO

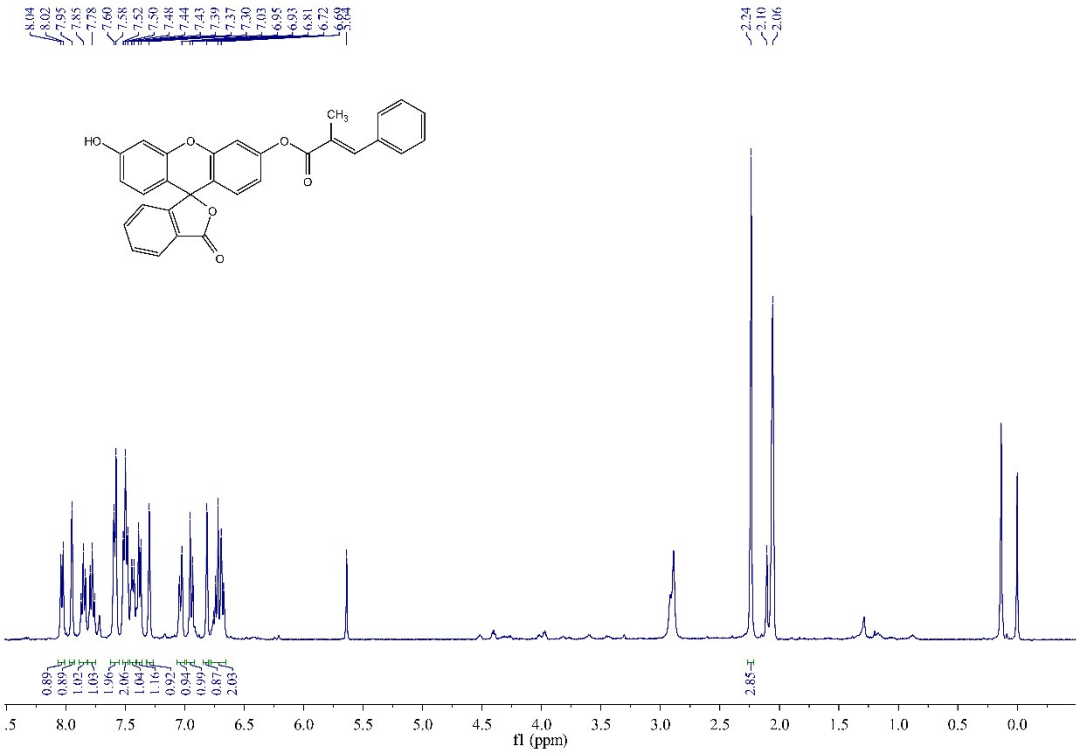

Figure S34. ^{1}H NMR of Fl-α-Me in $(CD_3)_2CO$

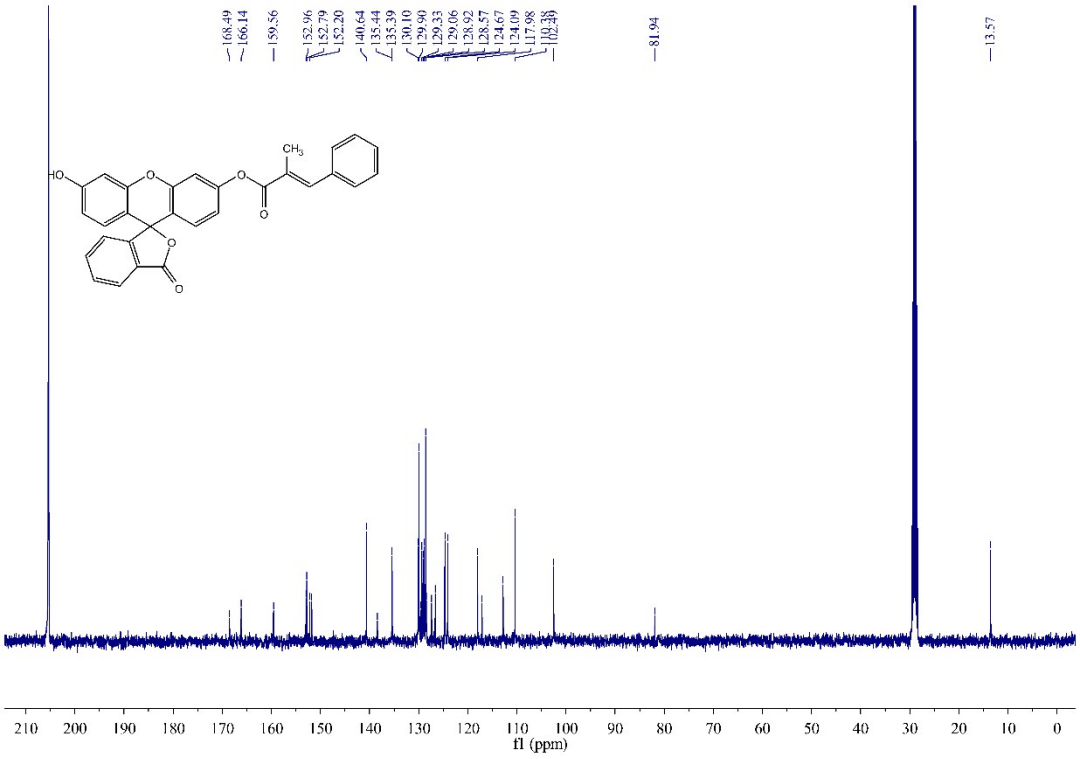

Figure S35. ^{13}C NMR of Fl-α-Me in $(CD_3)_2CO$

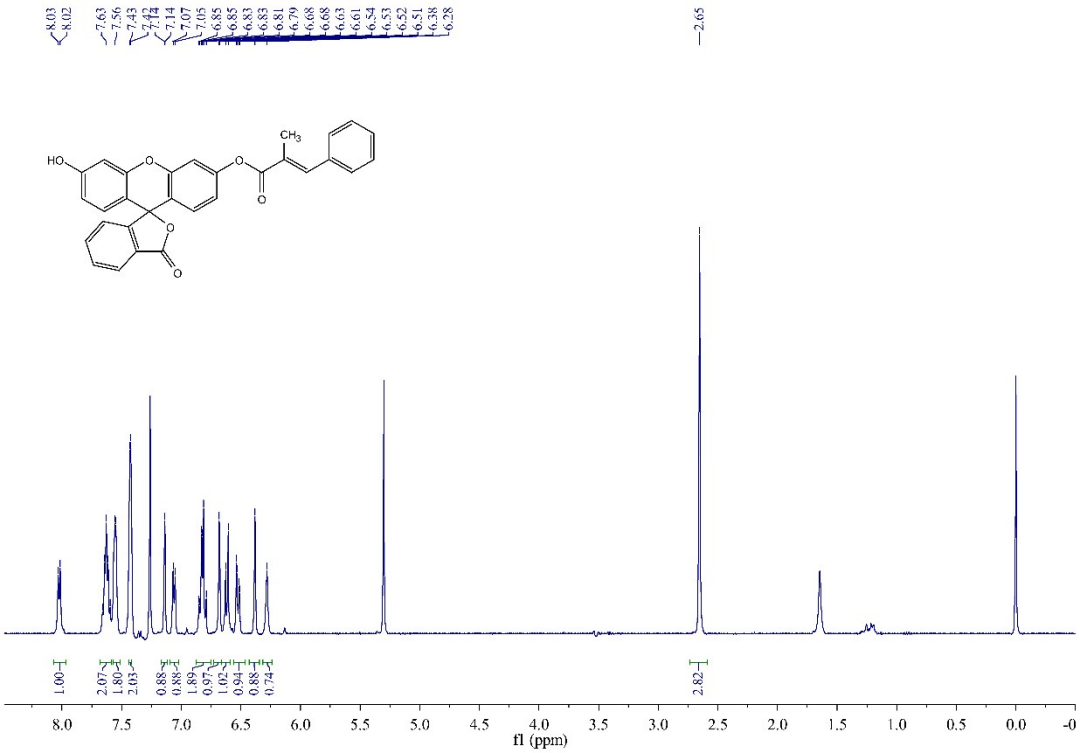

Figure S36. ^{1}H NMR of Fl-*β*-Me in $CDCl_3$

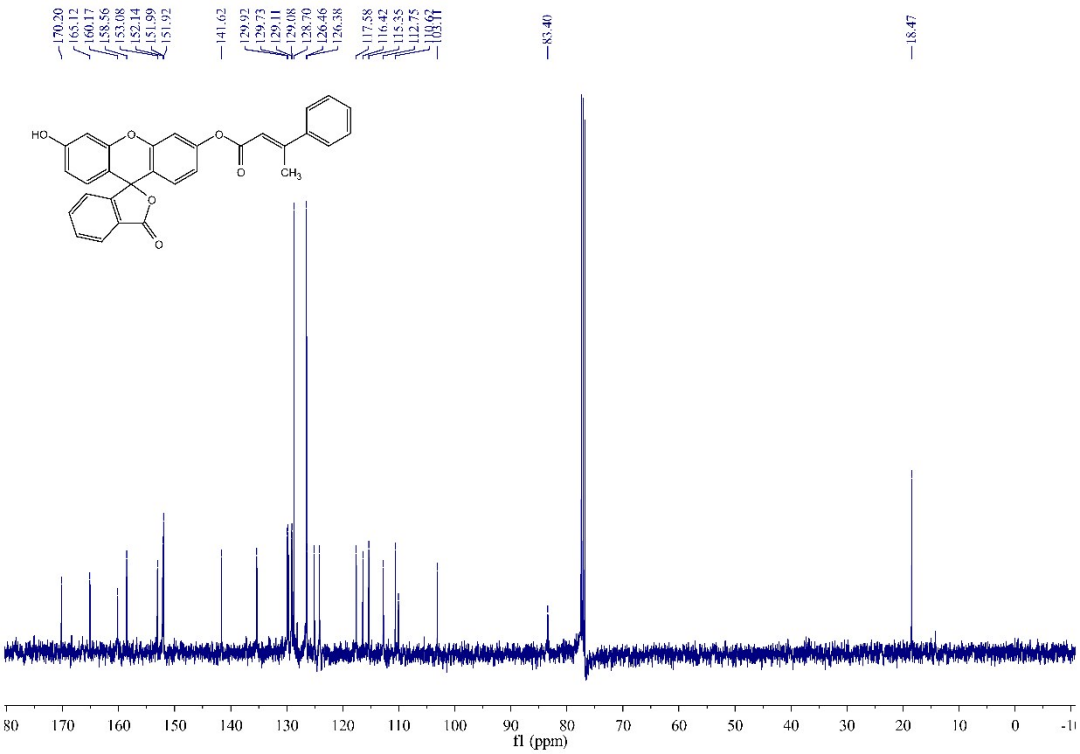

Figure S37. ^{13}C NMR of Fl-*β*-Me in $CDCl_3$

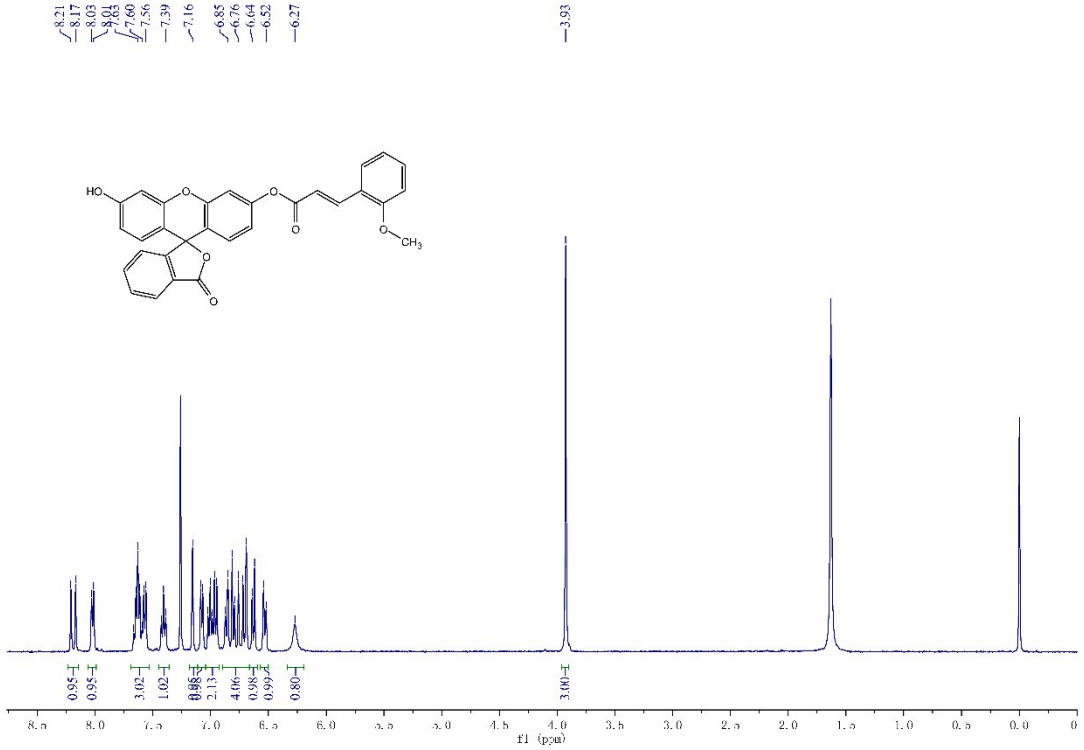

Figure S38. ^{1}H NMR of Fl-2OMe in $CDCl_3$

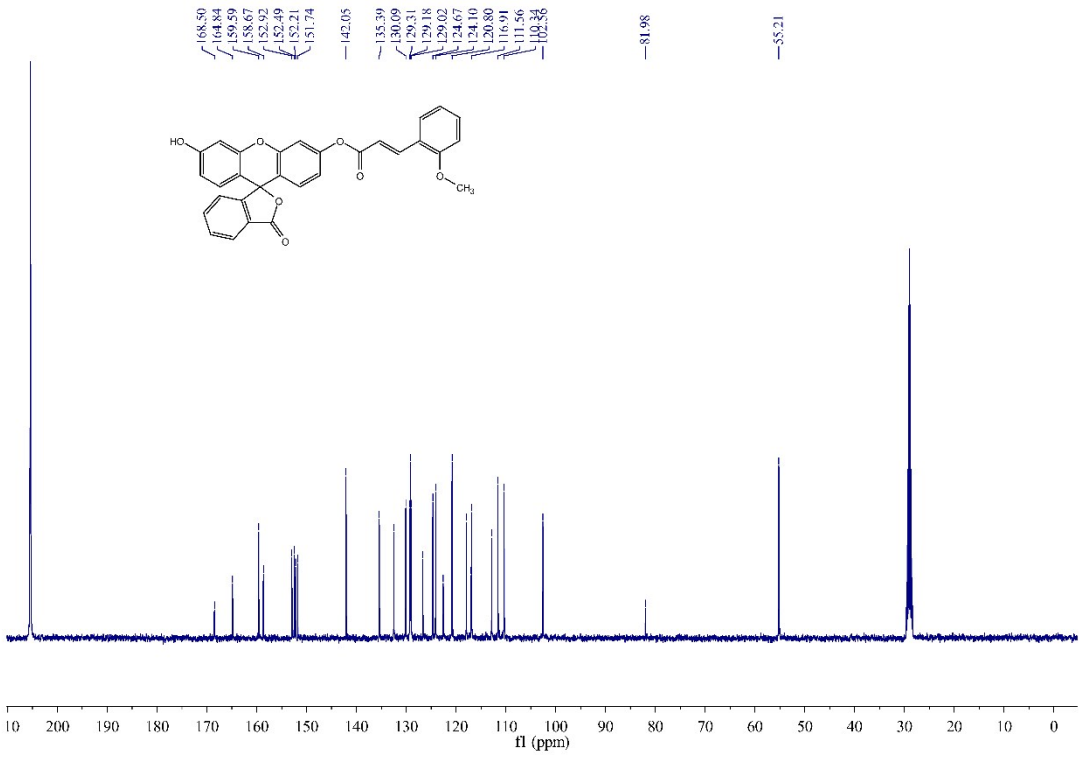

Figure S39. ^{13}C NMR of Fl-2OMe in $(CD_3)_2CO$

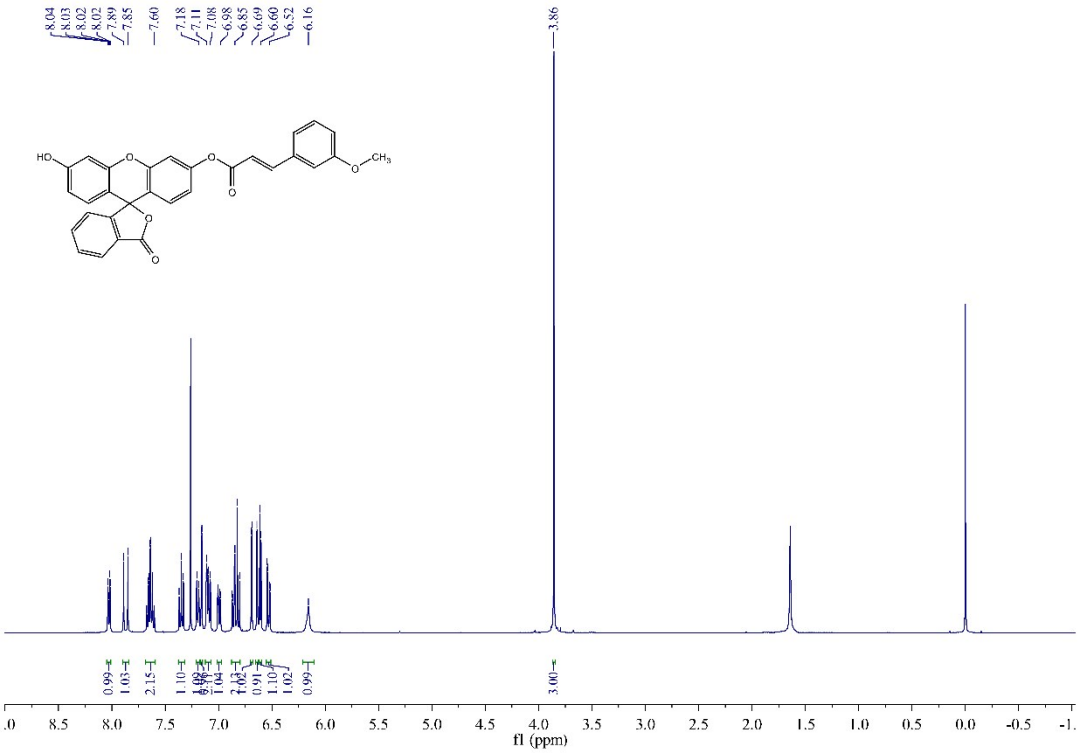

Figure S40. ^{1}H NMR of Fl-3OMe in $CDCl_3$

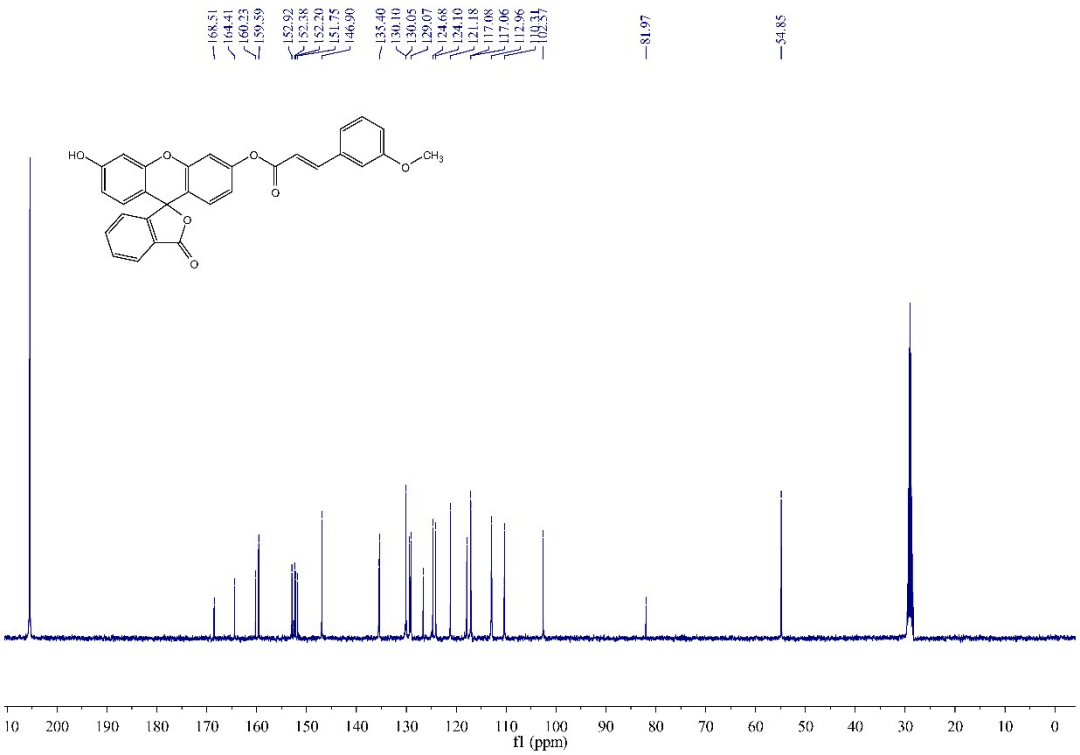

Figure S41. ^{13}C NMR of Fl-3OMe in $(CD_3)_2CO$

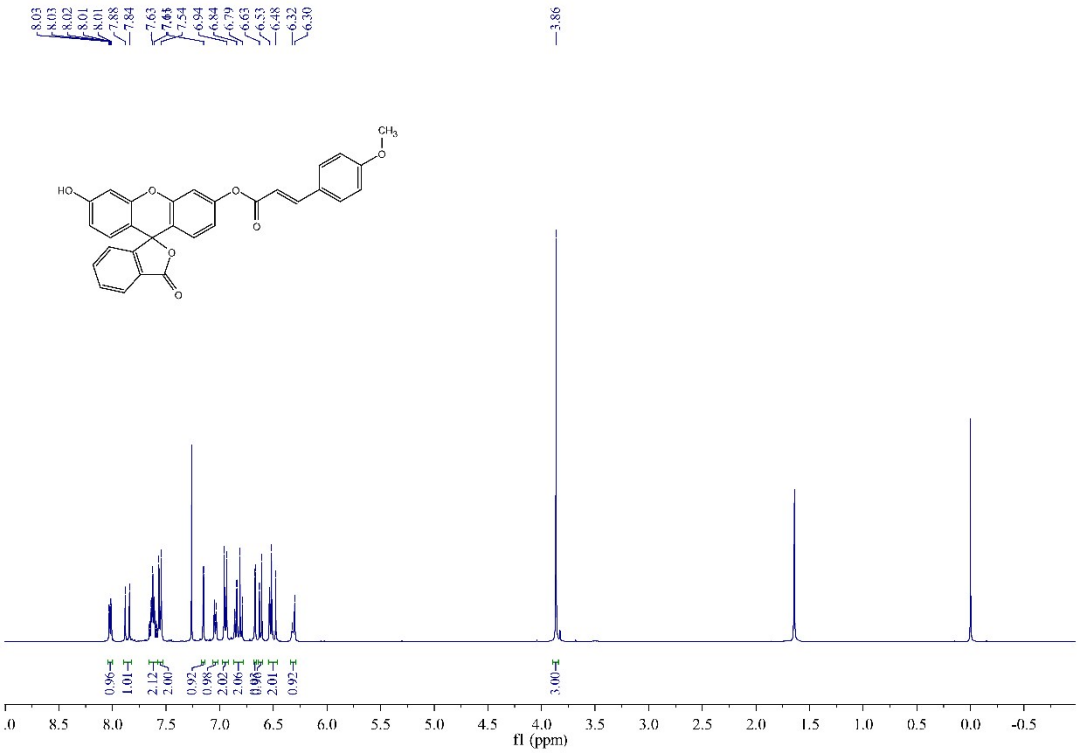

Figure S42. ^{1}H NMR of Fl-4OMe in $CDCl_3$

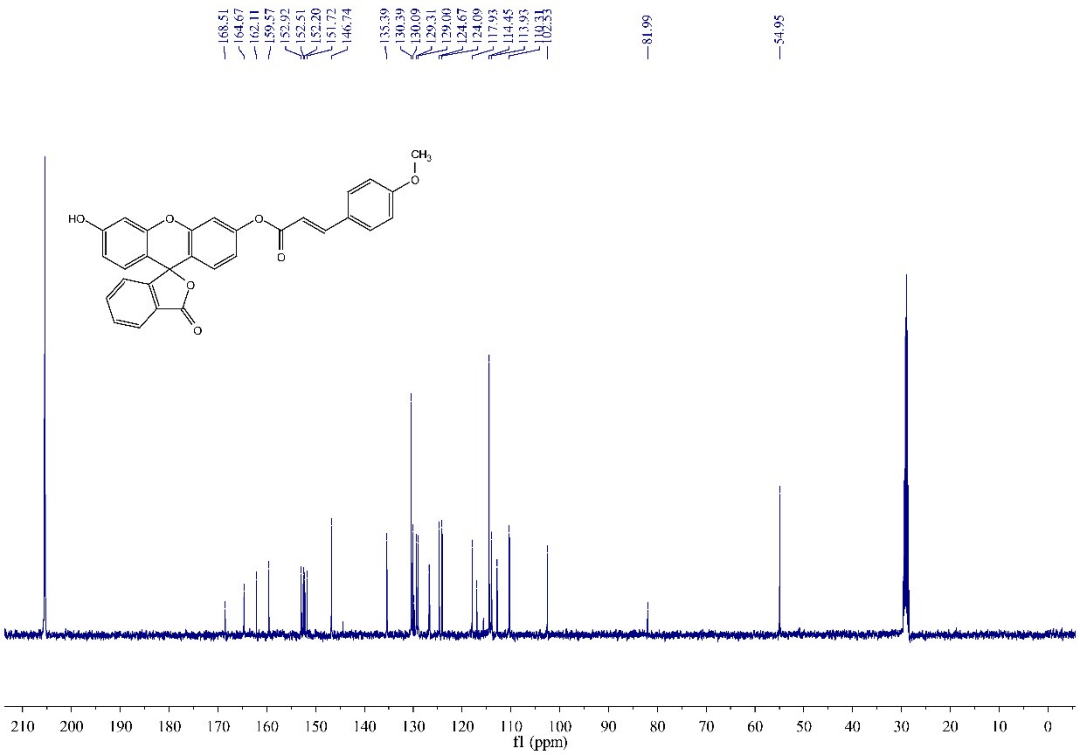

Figure S43. ^{13}C NMR of Fl-4OMe in $(CD_3)_2CO$

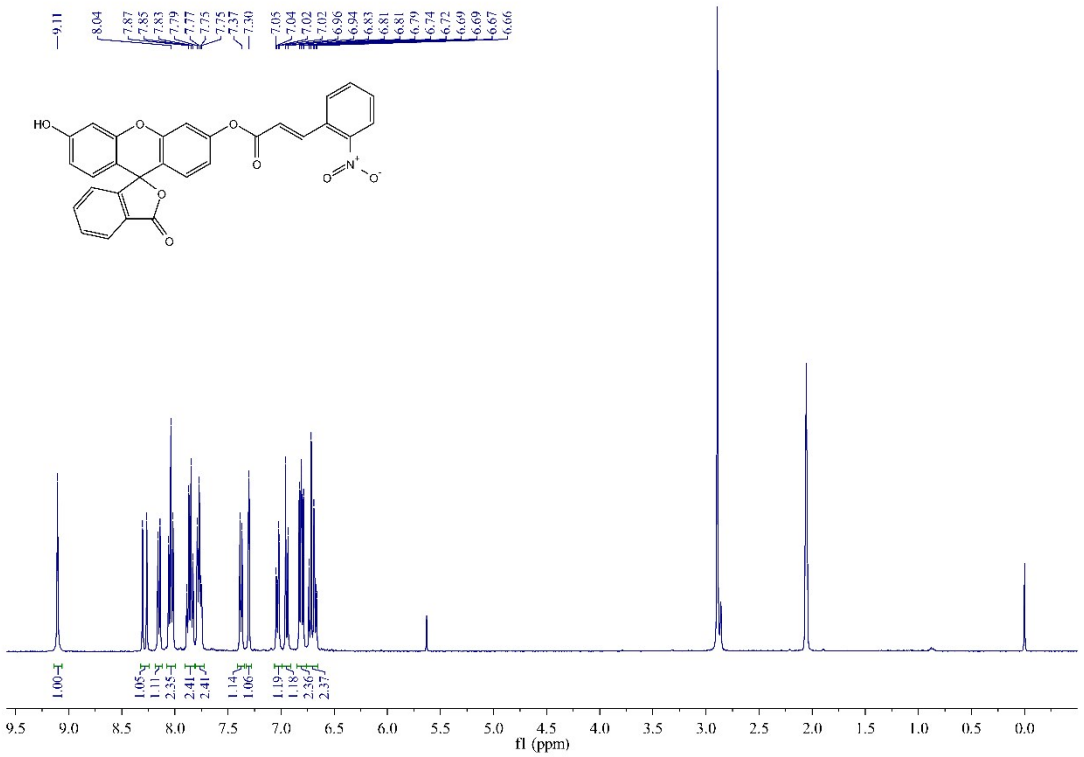

Figure S44. ^{1}H NMR of Fl-2NO$_2$ in (CD$_3$)$_2$CO

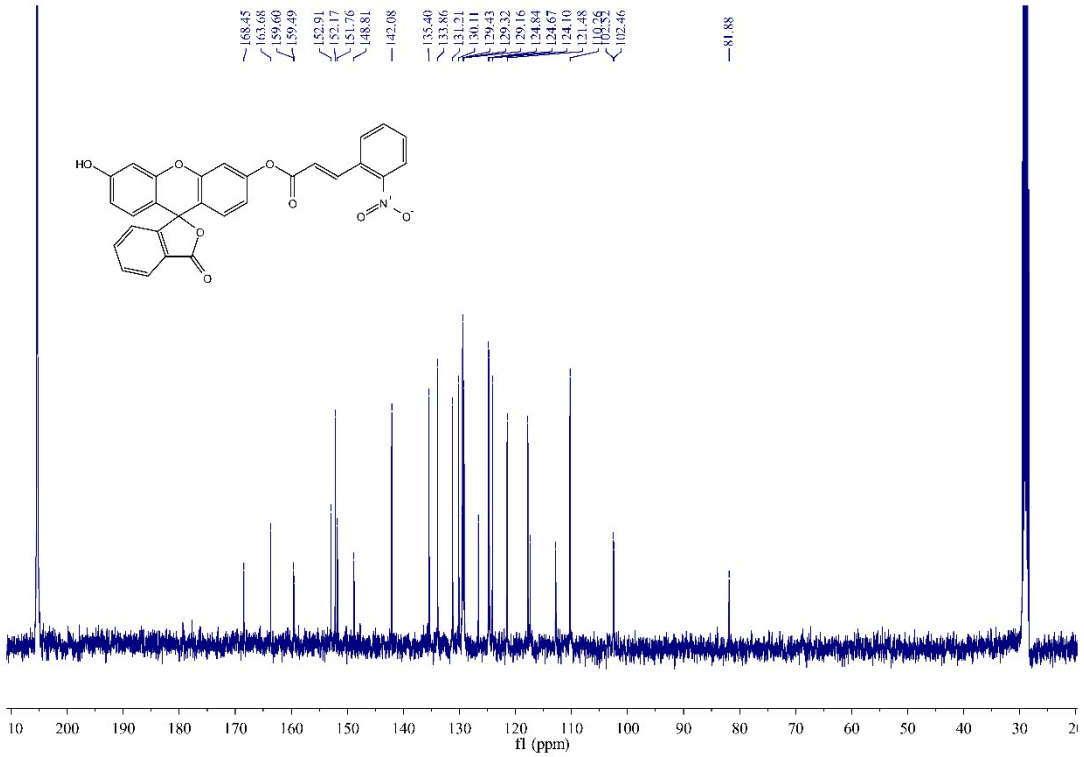

Figure S45. ^{13}C NMR of Fl-2NO$_2$ in (CD$_3$)$_2$CO

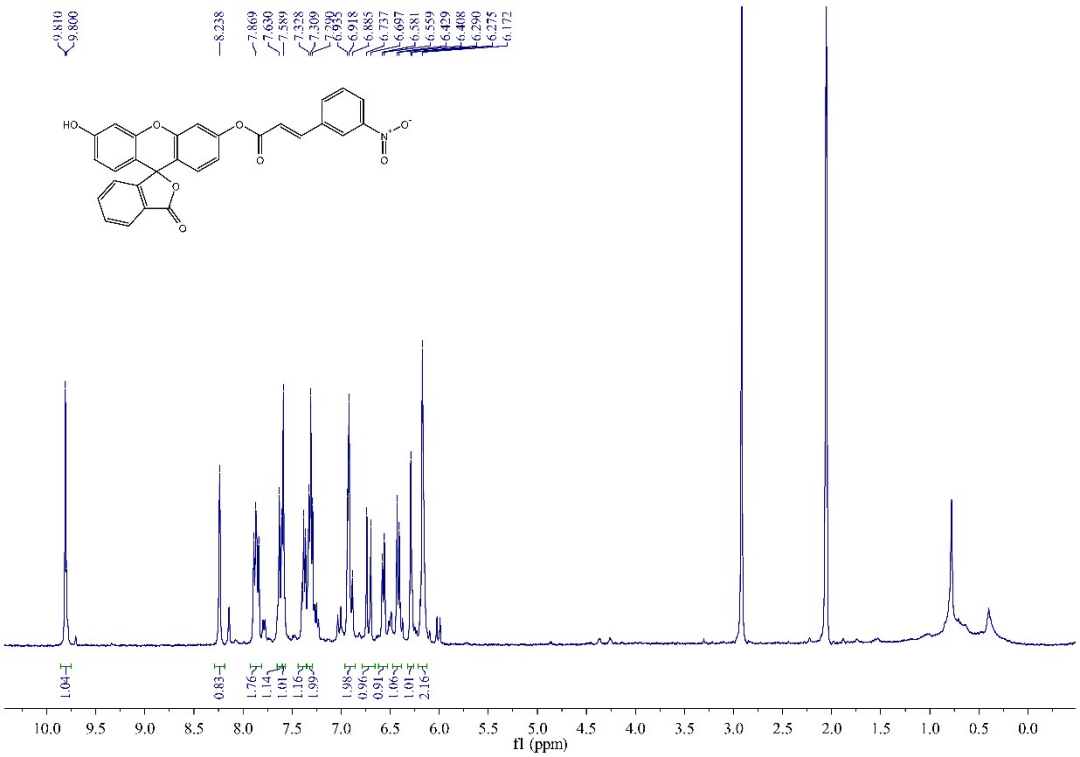

Figure S46. ^{1}H NMR of Fl-3NO$_2$ in (CD$_3$)$_2$CO

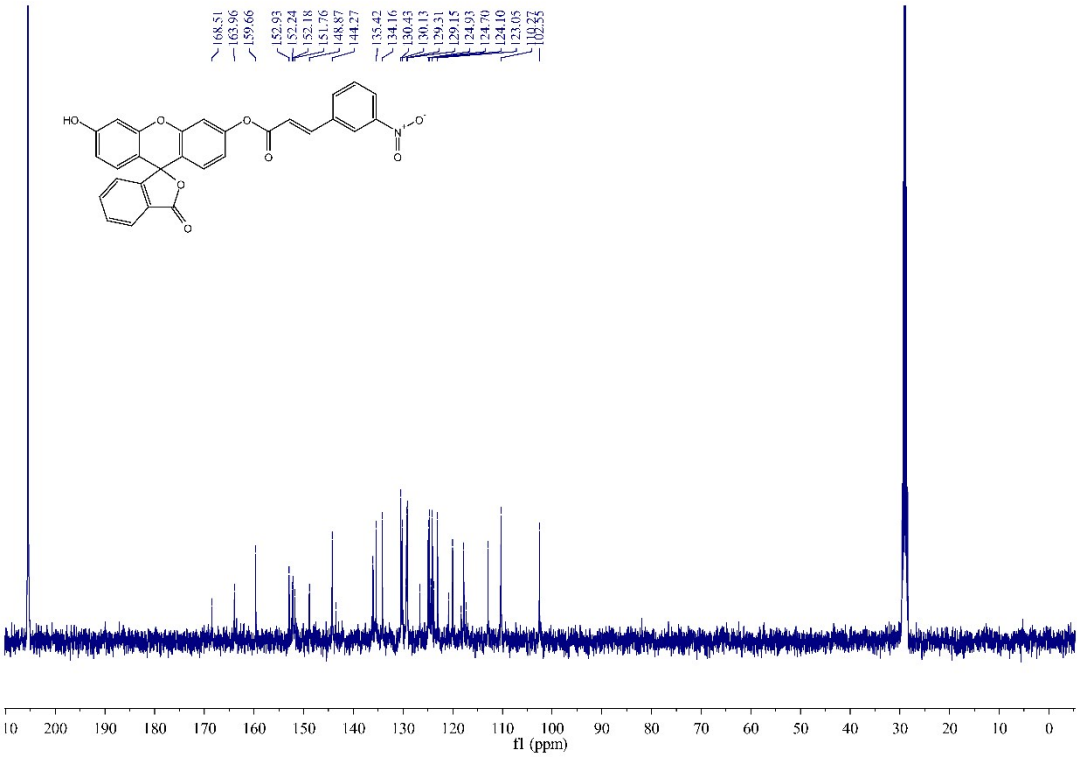

Figure S47. ^{13}C NMR of Fl-3NO$_2$ in (CD$_3$)$_2$CO

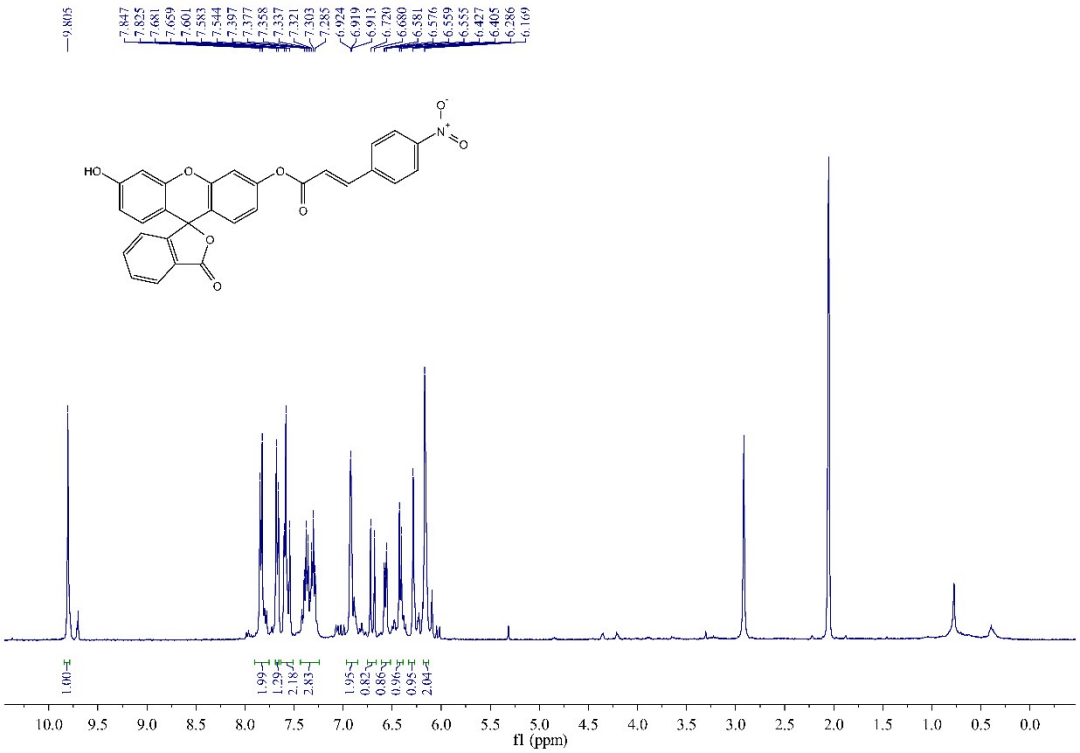

Figure S48. ^{1}H NMR of Fl-4NO$_2$ in d^6-DMSO

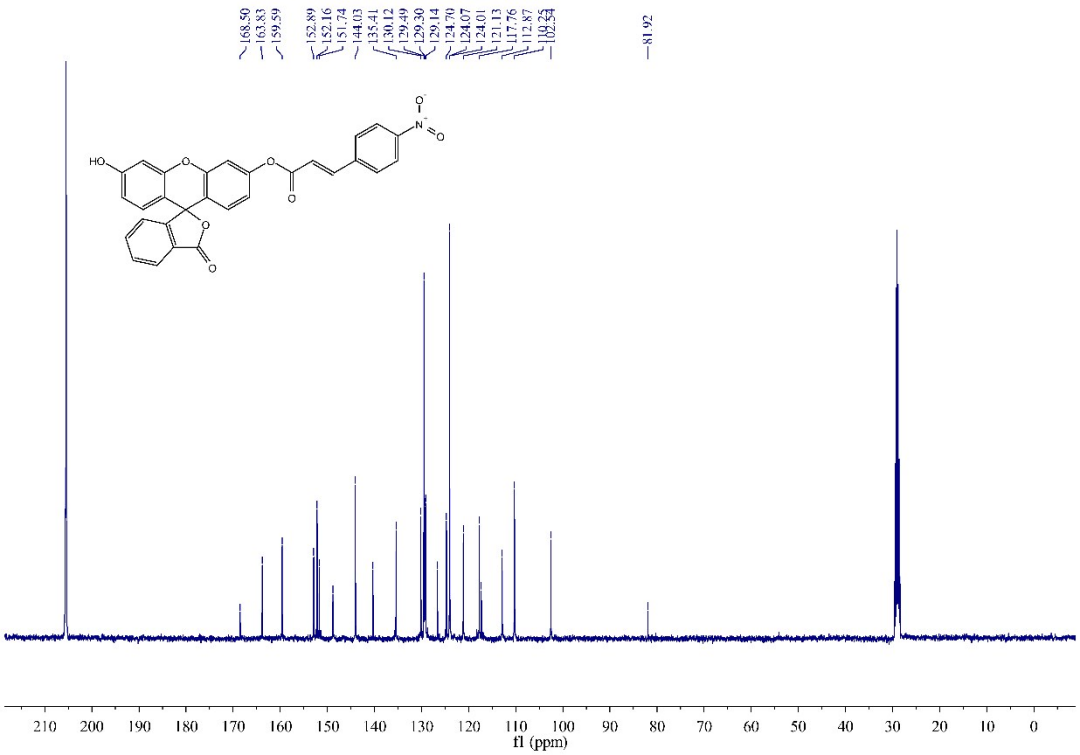

Figure S49. ^{13}C NMR of Fl-4NO$_2$ in d^6-DMSO

7.2 HRMS spectra of all probes

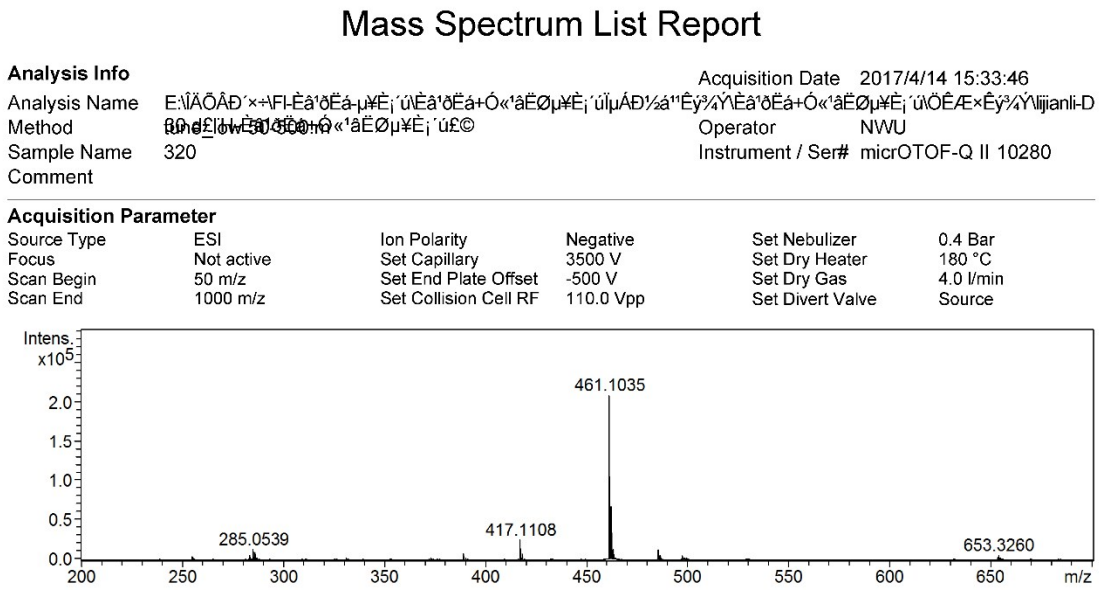

Figure S50. HRMS spectra of **Fl-H**

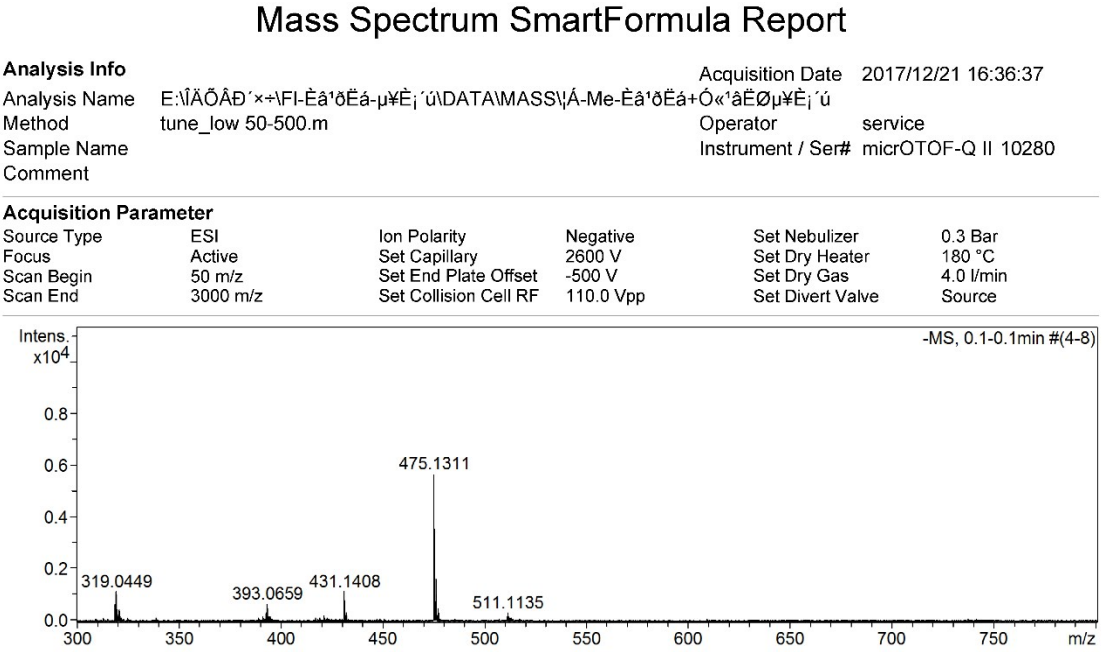

Figure S51. HRMS spectra of **Fl-α-Me**

Mass Spectrum List Report

Analysis Info

Analysis Name	C:\Users\lenovo\Desktop\lijianli-20171107-D6.d	Acquisition Date	2017/11/7 15:47:52
Method	tune_low 50-500.m	Operator	service
Sample Name		Instrument / Ser#	micrOTOF-Q II 10280
Comment			

Acquisition Parameter

Source Type	ESI	Ion Polarity	Negative	Set Nebulizer	0.3 Bar
Focus	Active	Set Capillary	2600 V	Set Dry Heater	180 °C
Scan Begin	50 m/z	Set End Plate Offset	-500 V	Set Dry Gas	4.0 l/min
Scan End	3000 m/z	Set Collision Cell RF	110.0 Vpp	Set Divert Valve	Source

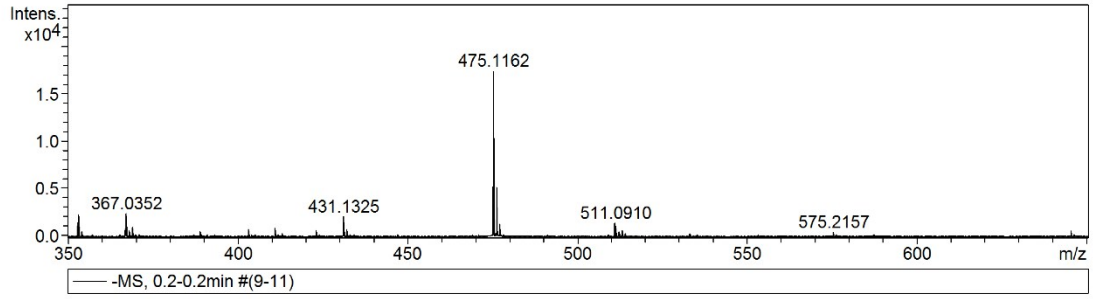

Figure S52. HRMS spectra of **Fl-*β*-Me**

Mass Spectrum List Report

Analysis Info

Analysis Name	E:\ÎÄÕÂÐ´×÷\Fl-Èâ¹ðËá-µ¥È¡´ú\Èâ¹ðËá+Ó«¹âËØµ¥È¡´úÏµÁÐ½á¹¹Êý¾Ý\2-OMeÈâ¹ðËá+Ó«¹âËØµ¥È¡´ú\ÖÊÆ×Êý¾Ý\	Acquisition Date	2016/10/21 10:29:44
Method	[illegible]Fluµ¥\lijl-wangzhaohui-D7.d	Operator	NWU
Sample Name	20160622	Instrument / Ser#	micrOTOF-Q II 10280
Comment			

Acquisition Parameter

Source Type	ESI	Ion Polarity	Negative	Set Nebulizer	0.4 Bar
Focus	Not active	Set Capillary	3500 V	Set Dry Heater	180 °C
Scan Begin	50 m/z	Set End Plate Offset	-500 V	Set Dry Gas	4.0 l/min
Scan End	3000 m/z	Set Collision Cell RF	110.0 Vpp	Set Divert Valve	Source

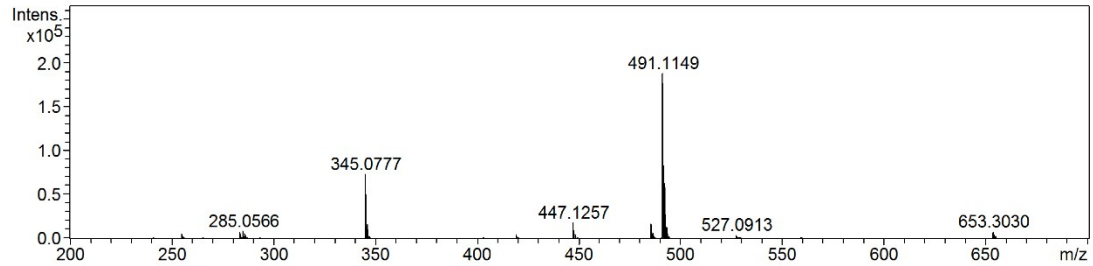

Figure S53. HRMS spectra of **Fl-2OMe**

Mass Spectrum List Report

Analysis Info

Analysis Name	E:\ÎÄÕÂÐ´×÷\Fl-Èâ¹ðËá-µ¥È¡´ú\Èâ¹ðËá+Ó«¹âËØµ¥È¡´úÏµÁÐ½á¹¹Êý¾Ý\3-OMeÈâ¹ðËá+Ó«¹âËØµ¥È¡´ú\ÖÊÆ×Êý¾Ý\	Acquisition Date	2016/10/21 10:31:13
Method	[illegible]Fluµ¥\lijl-wangzhaohui-D8.d	Operator	NWU
Sample Name	20160622	Instrument / Ser#	micrOTOF-Q II 10280
Comment			

Acquisition Parameter

Source Type	ESI	Ion Polarity	Negative	Set Nebulizer	0.4 Bar
Focus	Not active	Set Capillary	3500 V	Set Dry Heater	180 °C
Scan Begin	50 m/z	Set End Plate Offset	-500 V	Set Dry Gas	4.0 l/min
Scan End	3000 m/z	Set Collision Cell RF	110.0 Vpp	Set Divert Valve	Source

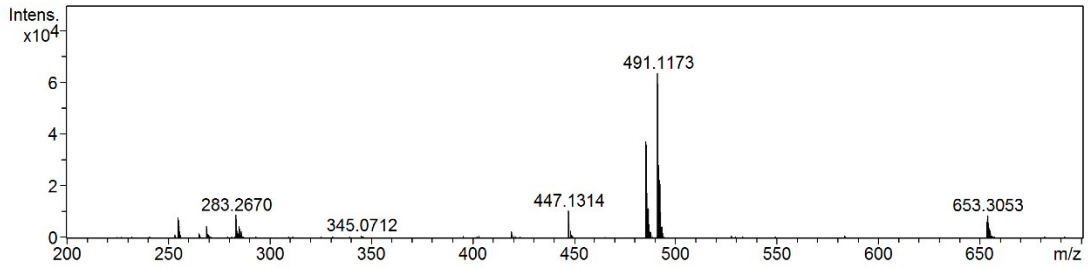

Figure S54. HRMS spectra of **Fl-3OMe**

Mass Spectrum List Report

Analysis Info

Analysis Name	E:\ÎÄÕÂÐ´×÷\Fl-Èâ¹ðËá-µ¥È¡´ú\Èâ¹ðËá+Ó«¹âËØµ¥È¡´úÏµÁÐ½á¹¹Êý¾Ý\4-OMeÈâ¹ðËá+Ó«¹âËØµ¥È¡´ú\ÖÊÆ×Êý¾Ý\j	Acquisition Date	2017/3/10 15:34:16
Method	t_liuyanqun-D29.d	Operator	NWU
Sample Name	< No Sample >	Instrument / Ser#	micrOTOF-Q II 10280
Comment			

Acquisition Parameter

Source Type	ESI	Ion Polarity	Negative	Set Nebulizer	0.4 Bar
Focus	Not active	Set Capillary	3500 V	Set Dry Heater	180 °C
Scan Begin	50 m/z	Set End Plate Offset	-500 V	Set Dry Gas	4.0 l/min
Scan End	3000 m/z	Set Collision Cell RF	110.0 Vpp	Set Divert Valve	Source

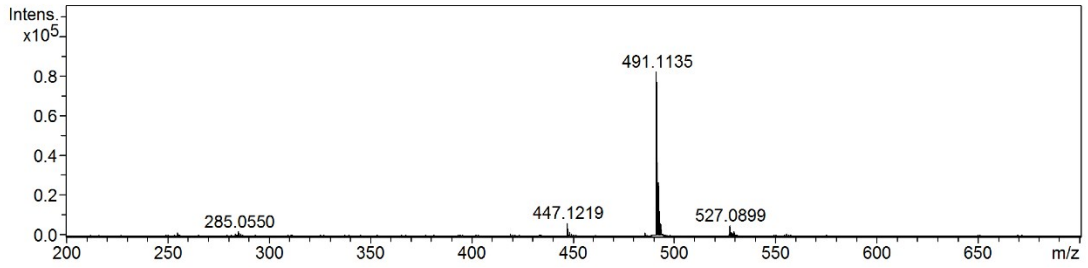

Figure S55. HRMS spectra of **Fl-4OMe**

Mass Spectrum List Report

Analysis Info

Analysis Name	E:\ÎÄÕÂÐ´×÷\Fl-Èâ¹ðËá-µ¥È¡´ú\DATA\MASS\2-NO2-Èâ¹ðËá+Ó«¹âËØµ¥È¡´ú\ljl-Liquanquan-2-Ïõ»ù-µ¥.d	Acquisition Date	2017/5/22 11:29:43
Method	tune_low 50-500.m	Operator	NWU
Sample Name		Instrument / Ser#	micrOTOF-Q II 10280
Comment			

Acquisition Parameter

Source Type	ESI	Ion Polarity	Negative	Set Nebulizer	0.4 Bar
Focus	Not active	Set Capillary	3500 V	Set Dry Heater	180 °C
Scan Begin	50 m/z	Set End Plate Offset	-500 V	Set Dry Gas	4.0 l/min
Scan End	1000 m/z	Set Collision Cell RF	110.0 Vpp	Set Divert Valve	Source

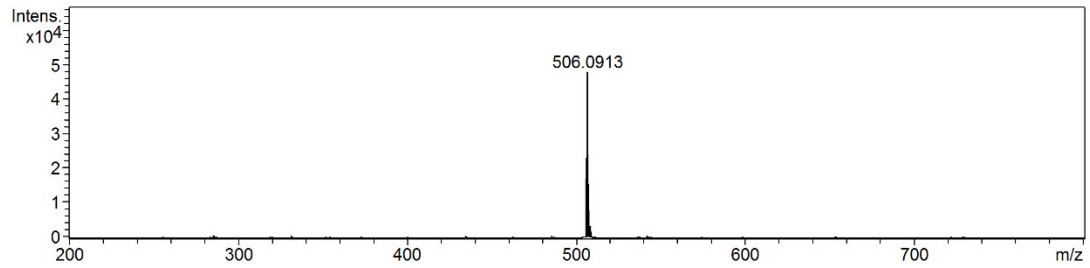

Figure S56. HRMS spectra of **Fl-2NO$_2$**

Mass Spectrum List Report

Analysis Info

Analysis Name	E:\ÎÄÕÂÐ´×÷\Fl-Èâ¹ðËá-µ¥È¡´ú\DATA\MASS\3-NO2-Èâ¹ðËá+Ó«¹âËØµ¥È¡´ú\ljl-Liquanquan-B22-3NO2-µ¥.d	Acquisition Date	2017/5/22 11:31:11
Method	tune_low 50-500.m	Operator	NWU
Sample Name		Instrument / Ser#	micrOTOF-Q II 10280
Comment			

Acquisition Parameter

Source Type	ESI	Ion Polarity	Negative	Set Nebulizer	0.4 Bar
Focus	Not active	Set Capillary	3500 V	Set Dry Heater	180 °C
Scan Begin	50 m/z	Set End Plate Offset	-500 V	Set Dry Gas	4.0 l/min
Scan End	1000 m/z	Set Collision Cell RF	110.0 Vpp	Set Divert Valve	Source

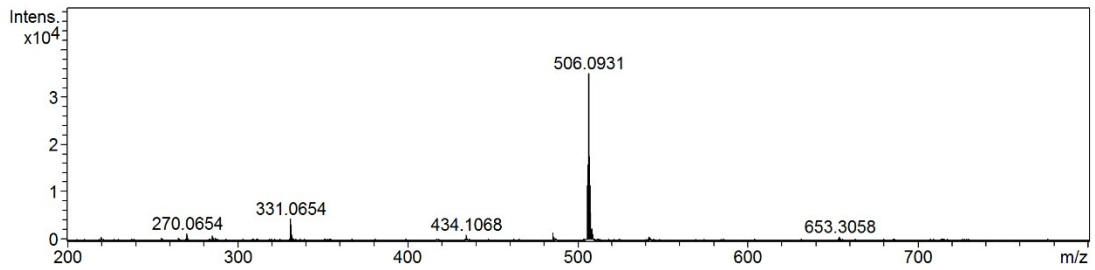

Figure S57. HRMS spectra of **Fl-3NO$_2$**

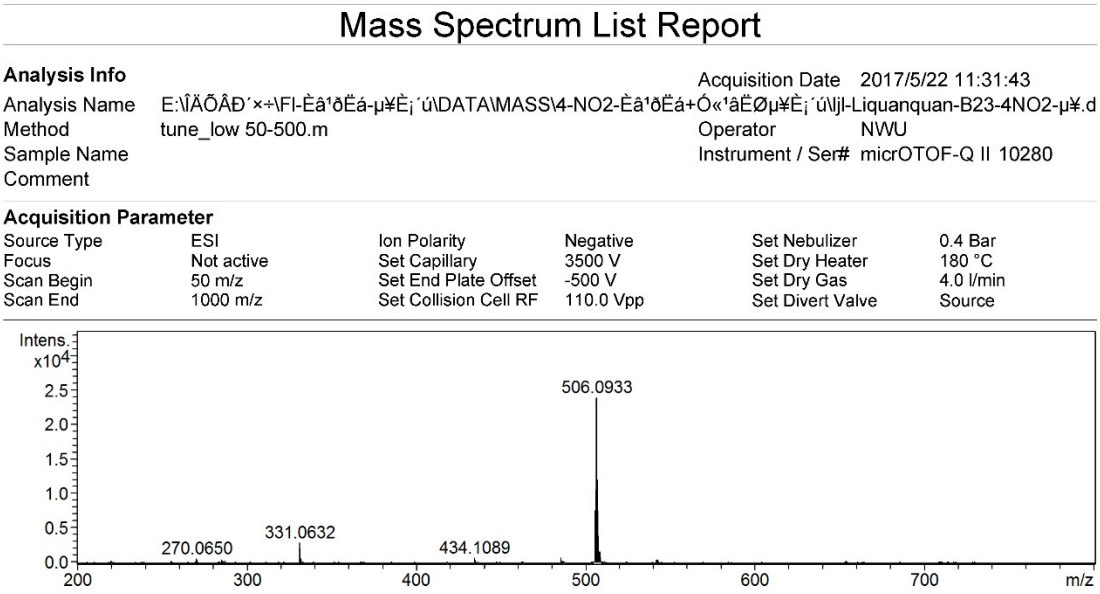

Figure S58. HRMS spectra of **Fl-4NO$_2$**

References:

1. Becke, A. D., Density-functional thermochemistry. III. The role of exact exchange. *Journal of Chemical Physics* **1993,** *98* (7), 5648.

2. Frisch, M. J.; Trucks, G. W.; Schlegel, H. B.; Scuseria, G. E.; Robb, M. A.; Cheeseman, J. R.; Scalmani, G.; Barone, V.; Mennucci, B.; Petersson, G. A.; Nakatsuji, H.; Caricato, M.; Li, X.; Hratchian, H. P.; Izmaylov, A. F.; Bloino, J.; Zheng, G.; Sonnenberg, J. L.; Hada, M.; Ehara, M.; Toyota, K.; Fukuda, R.; Hasegawa, J.; Ishida, M.; Nakajima, T.; Honda, Y.; Kitao, O.; Nakai, H.; Vreven, T.; Montgomery Jr., J. A.; Peralta, J. E.; Ogliaro, F.; Bearpark, M. J.; Heyd, J.; Brothers, E. N.; Kudin, K. N.; Staroverov, V. N.; Kobayashi, R.; Normand, J.; Raghavachari, K.; Rendell, A. P.; Burant, J. C.; Iyengar, S. S.; Tomasi, J.; Cossi, M.; Rega, N.; Millam, N. J.; Klene, M.; Knox, J. E.; Cross, J. B.; Bakken, V.; Adamo, C.; Jaramillo, J.; Gomperts, R.; Stratmann, R. E.; Yazyev, O.; Austin, A. J.; Cammi, R.; Pomelli, C.; Ochterski, J. W.; Martin, R. L.; Morokuma, K.; Zakrzewski, V. G.; Voth, G. A.; Salvador, P.; Dannenberg, J. J.; Dapprich, S.; Daniels, A. D.; Farkas, Ö.; Foresman, J. B.; Ortiz, J. V.; Cioslowski, J.; Fox, D. J. *Gaussian 09*, Gaussian, Inc.: Wallingford, CT, USA, 2009.